國 立 交 通 大 學

電信工程學系

博 士 論 文

基於諧振與同調觀點之血液壓力波分析

Analysis of Blood Pressure Wave Based on
the Viewpoint of Resonance and Coherence

研究生：魏清泉

指導教授：吳霖堃
共同指導教授：羅佩禎

中 華 民 國 九 十 五 年 一 月

基於諧振與同調觀點之血液壓力波分析

Analysis of Blood Pressure Wave Based on the Viewpoint of Resonance and Coherence

研究生：魏清泉　　　　　　　　Student : Ching-Chuan Wei

指導教授：吳霖堃　　　　　　　Advisor : Lin-Kun Wu
共同指導教授：羅佩禎　　　　　Co-advisor : Pei-Chen Lo

國 立 交 通 大 學
電 信 工 程 學 系
博 士 論 文

Submitted to Department of Communication Engineering
College of Electrical Engineering and Computer Science
National Chiao Tung University
in Partial Fulfillment of the Requirements
for the Degree of
Doctor of Philosophy
in
Communication Engineering
January 2006
Hsinchu, Taiwan, Republic of China

中 華 民 國 九 十 五 年 一 月

基於諧振與同調觀點之血液壓力波分析

國 立 交 通 大 學　電信工程學系

研究生：魏清泉　　　　　　　　　　　　指導教授 ： 吳霖堃
　　　　　　　　　　　　　　　　　　　共同指導教授 ：羅佩禎

摘要

　　在這篇論文中我們提出一個新的觀點來分析血液循環，也就是將血液循環系統視為一個電訊號激發的機械振動系統，並且用一個以橫向振動為主的血液壓力波方程式來描述血液循環時的諧振現象，接著我們把ECG與BPW(血液壓力波)視為此系統的輸入與輸出，並探討它的頻域特性，首先我們發現對於健康的受測者，其ECG與BPW的功率頻譜有相當大的重疊，頻譜耦合係數(Spectral coupling coefficient)趨近於1，而心血管相關疾病的患者則有較大的差異，頻譜耦合係數小於1，此乃因為健康者的動脈系統彈性極佳，能將心臟搏動的頻率變化完整地耦合至動脈系統，也就是心臟與動脈系統發生諧振；而心血管相關疾病的患者，則因動脈系統彈性較差或其它阻力而無法完整地耦合心臟搏動的頻率到動脈系統，其諧振特性較差；另一方面，其三階頻譜(Bicoherence) 趨近於1，顯示對於健康的受測者，其ECG與BPW有較強的相位耦合，而心血管相關疾病的患者其相位耦合則較弱；此外健康的受測者其轉移函數(Transfer function)也較心血管相關疾病的患者有較平坦的曲線，這些結果都顯示健康者的動脈系統彈性較心血管相關疾病的患者好。我們也建立此系統的頻域電路模型，並計算其諧振品質因素，結果顯示健康的受測者有較高的諧振品質因素。

　　此外 ECG 的頻率調變及振幅調變效應、血管壁的欠阻尼與過阻尼效應也被探討，在輸入的電刺激信號與輸出的血管壁振動信號間，我們計算其同調函數(Coherence function) ，因此我們可以計算輸入(心臟) 與輸出(動脈系統) 間同調

及干擾的程度，前五個諧波的平均同調值被用來衡量同調的程度，實驗結果顯示健康的受測者其平均同調值趨近於1，同調的程度較心血管相關疾病的患者高，也就是干擾的程度較小，根據上述這些觀念，我們得以建立一個血液循環的系統模型。

最後我們研究靜坐前後對心血管循環系統時域特性的影響，我們觀察 BPW 中 P 波的上升斜率、T 波的高度、降中峽的高度、D 波的高度等參數，實驗結果顯示實驗組(靜坐者)的 P 波的上升斜率、T 波及 D 波的高度皆較控制組明顯地 ($P<0.05$)增加而降中峽的高度明顯地減少，顯示經由靜坐的訓練能使心血管循環系統的特性有明顯地改善。

Analysis of Blood Pressure Wave Based on the Viewpoint of Resonance and Coherence

Department of Communication Engineering

National Chiao Tung University

Student : Ching-Chuan Wei **Advisor : Lin-Kun Wu**

Co-advisor : Pei-Chen Lo

Abstract

In this dissertation, we presented a novel idea for analyzing blood circulation that is viewed as an electrically-driven, mechanical-pumping mechanism. Besides, a blood pressure wave equation (BPW)with radial dilation is used to describe the resonance effect in blood circulation. Considering the ECG (electrocardiograph) and BPW as the input and output signals of the system, we aim to apply the spectral analysis approach for evaluating the property of blood circulation from the viewpoint of resonance and coherence. First, the power spectrum of the ECG coincides well with that of the BPW for healthy subjects, but deviates significantly from the BPW's for vascular patients. According to the results, we may infer that the artery wall of healthy subjects exhibits better elasticity of artery wall for healthy subjects than that of cardiovascular-related patients. Thus, the spectrum of ECG can be completely coupled to BPW's. In other words, heart resonates with the arterial system. Second, bispectral analysis

demonstrates a strong phase coupling between ECG and BPW for the healthy subjects and a weaker coupling for subjects with vascular problems. Third, the transfer function for healthy subjects exhibits a flatter magnitude than that for patients. All the results demonstrate that healthy subjects possess better artery elasticity for healthy subjects than that for cardiovascular patients. In addition, we propose a resonance circuit model in frequency domain to characterize the behavior of blood circulation. The quality factor of a healthy model also reveals better resonance characteristic than the one of an abnormal model.

In addition, this thesis presents the results of investigating the FM (frequency modulation) and AM (amplitude modulation) effects on ECG, as well as the under-damping and over-damping effects in the blood circulation system are studied. Coherence function is used to measure the degree of BPW in resonance with ECG, from which perturbations of the system can be determined. System model based on the above concepts is accordingly established. The average of the first five peaks (S) is used to quantify the power coherence effect. The evaluated p-value (< 0.01) reveals that the distinction of power coherence between the healthy subjects and cardiovascular patients is significant. Consequently, we conclude that if the S approaches a value close to one, the output is almost completely attributed to the input. In the case, the system's operation involves fewer perturbation signals so that the cardiovascular system will remain in a better condition. Conversely, if S is much below one, the cardiovascular system operates under high perturbation and tends to decay or become diseased.

Finally, we study the effect of Zen meditation on the characteristics of cardiovascular system, mainly based on the time-domain features of blood pressure

waveform. Four parameters derived from the BPW include the rising slope ($\frac{h_1}{t_1}$) of P

wave, the normalized height of T wave ($\frac{h_3}{h_1}$), the normalized height of V_3 valley

($\frac{h_4}{h_1}$), and the normalized height of D wave ($\frac{h_5}{h_1}$), where t_1 and h_i, $i = 1, \ldots, 5$ are

quantitative features of the BPW waveform pattern. A larger value of $\frac{h_1}{t_1}$ reflects

better heart ejection ability and aorta compliance. A larger value of $\frac{h_3}{h_1}$ may infer an

arterial system with good elasticity. The decrease (increase) of $\frac{h_4}{h_1}$ parameter

indicates the decrease (increase) of peripheral resistance of vessels. A larger value of

$\frac{h_5}{h_1}$ indicates the better artery elasticity and aortic valve function. In comparison with

the control group, Zen-meditation practitioners have the *post-meditation* $\frac{h_1}{t_1}$, $\frac{h_3}{h_1}$,

and $\frac{h_5}{h_1}$ increase more, while $\frac{h_4}{h_1}$ decrease more, with statistical significance

($P<0.05$). The observation allows us to infer that Zen meditation effectively improves

some important characteristics relevant to the health condition of cardiovascular

system.

誌謝

　　深深地感謝羅佩禎教授及吳霖堃教授的指導與協助，使得這篇論文得以完成與呈現。同時也感謝與沈慧宇老師的討論，激發我的想法；感謝黃瑞彬教授與劉裕永教授的協助；感謝生醫信號實驗室的夥伴們；也感謝那些曾拒絕我的論文的編輯者，他們讓我修正了很多觀點；感謝所有曾經與我同行的人。

　　最後，在寒冬的深夜裏，謝謝我摯愛的家人，麗卿、鵬倫、岳母與遠去的父親，你們的支持是我前進的動力。

TABLE OF CONTENTS

List of Figures

List of Tables

CHAPTER 1.   INTRODUCTION

1.1 Overview of Hemodynamics

The cardiovascular system is composed of the heart and blood vessels. They work together to form the blood-transporting system. Stimulated by ECG signal, the pumping of the heart constitutes the main force of oscillation, which thus forms a blood pressure wave (BPW) propagating along the arteries. With only 1.7 W power, an adult's heart pumps the blood to every part of the body, even up to the head, whose location is above the heart. Thus, there is no doubt that the cardiovascular system should develop a blood-transporting system with high efficiency to undertake the heavy load of blood transport.

In traditional hemodynamics, most studies such as Moens-Korteweg equation, Womersley equation, Windkessel model, etc., consider the blood flowing in longitudinal direction with static arterial wall (Fig. 1(a)), and the vibration of artery wall is just treated as a perturbation [1,2]. As a result, though the resonance effect had ever been proposed in blood circulation, McDonald supposed that resonance in arterial system is physically impossible due to the considerable damping of the reflected wave between reflection sites [1,2]. Actually, over 90% energy is stored in the vibration of arterial wall and less than 10% is stored in the longitudinal blood flow [1]. Traditional analysis ignored the potential energy caused by the transverse vibration of elastic arterial wall. It focuses concentrated on the kinetic energy generated by the axial momentum of blood flow. From the physiological viewpoint, the 180° bend at the arch of aorta converts the kinetic energy of blood flow into elastic potential energy of the artery wall as shown in Fig. 1(b). As a consequence, pressure wave originating from the transverse vibration of artery wall is generated,

that behaves like a transverse string wave (Fig. 1(c)).. Thus, resonance could be formed in transverse direction like an electromagnetic waveguide, and blood can flow in axial direction. Pressure wave transmission along artery makes energy transfer more efficient, that further reduces energy loss of making a turn. In addition, the vibration of artery wall squeezes the low axial blood flow so that the energy dissipated in viscosity is reduced.   Thus, wave of BPW may propagate along axial direction in the arterial system [3].

Therefore, Wang et al. presented the concept of "*resonance*" in the arterial system to facilitate the blood flowing into the organ. They also found that individual spectral harmonic of BPW corresponded to each specific organ [5-7]. They have conducted several experiments to verify this model. Furthermore, they proposed a concept of "*frequency matching*" to explain how organs were coupled with the heart [3]. They presumed that when the heart rate approached the natural frequency of arterial system, the circulatory system would have an optimal output for the pressure pulse and, therefore, the highest blood flow. The phenomenon is called the frequency matching and, in such a case, the entire system operated in its resonant state. The natural frequency depends on the structural properties of arterial system, the physiological states of blood vessels and blood, as well as the boundary conditions at vascular junctions, which can be changed by pathological factors. Consequently, under the frequency matching condition (resonance), organs receive blood from the heart more efficiently that makes them stay in a better physiological condition. This concept suggests that the alterations in the natural frequency can diminish the coupling efficiency from the heart to the arterial system and cause various diseases. Therefore, the analysis of frequency as well as of the phase relationship between the heart beat and arterial oscillation becomes an essential issue.

In addition, researchers have found that a specific organ may closely correspond to a specific spectral harmonic of the BPW. For example, the kidney, renal artery, and aorta combined show a coupled oscillation that is analogous to the resonance circuits, and the kidney vascular system exhibits a resonant frequency at the second harmonic of the BPW [7]. Thus, the abnormal value of the second spectral harmonic of BPW often relates to diseases of the kidney. Moreover, research results have revealed that the Chinese herbal drugs and acupuncture, which act on some specific organ, can also cause an amplitude variation of a corresponding spectral harmonic of the BPW [8,9]. These results further support the link between spectral harmonics of BPWs and the status of organs. Moreover, the respective close relationships between the first, third, as well as fourth spectral harmonics of the BPW and the liver, spleen, and lung have also been reported and investigated [9]. In summary, investigating of the spectrum of BPWs is valuable. However, the criterion used to judge the normality or abnormality of the spectral harmonics of BPWs is statistical and not objective. Therefore, comparison with the source signal (ECG) of the blood circulation system helps to identify the status of the cardiovascular system or organs on the basis of the BPW.

1.2 Viewpoint of this Research

In this study, we analyze the complex blood circulation system from the macroscopic system viewpoint. it is the first attempt that the blood circulation is regarded as an electrically-driven, mechanical-pumping mechanism, as demonstrated in Fig. 2(a) and 2(b). The ECG of lead Ⅱ and the BPW of the radial artery detected at the wrist are assumed to be the input and the output signals of the system, respectively, on the basis of the physiological point of view. This viewpoint is also similar to a motor in which the driving signal is electrical and the output torque is a mechanical

power that pumps a fluid.

In frequency domain analysis, we investigate the input-output relationship using power spectrum, bispectrum, transfer function and quality factor. Also, we proposed a frequency domain equivalent circuit to model the blood circulation. In addition, due to the elasticity of arterial wall, the major function of the arterial system is to transport energy via its transverse vibration. Thus, transverse resonance similar to the electromagnetic waveguide is formed and artery wall coherently oscillates with the excitation source. By coherence function, we analyze the coherence relationship between input and output, and establish a system model for blood circulation on the basis of the resonance theory and coherence power transfer. Eventually, the experiment of twenty-two healthy subjects and twenty-two cardiovascular-related patients are performed and analyzed by the above methods.

As to the time-domain analysis, we utilize some parameters of BPW such as the rising slope of P wave, height of T wave, D wave and V_3 valley (valley between T wave and D wave) to assess the status of cardiovascular system under meditation.

Artery wall

Pressure

(a)

Arch of Aorta

(b)

Artery wall

(c)
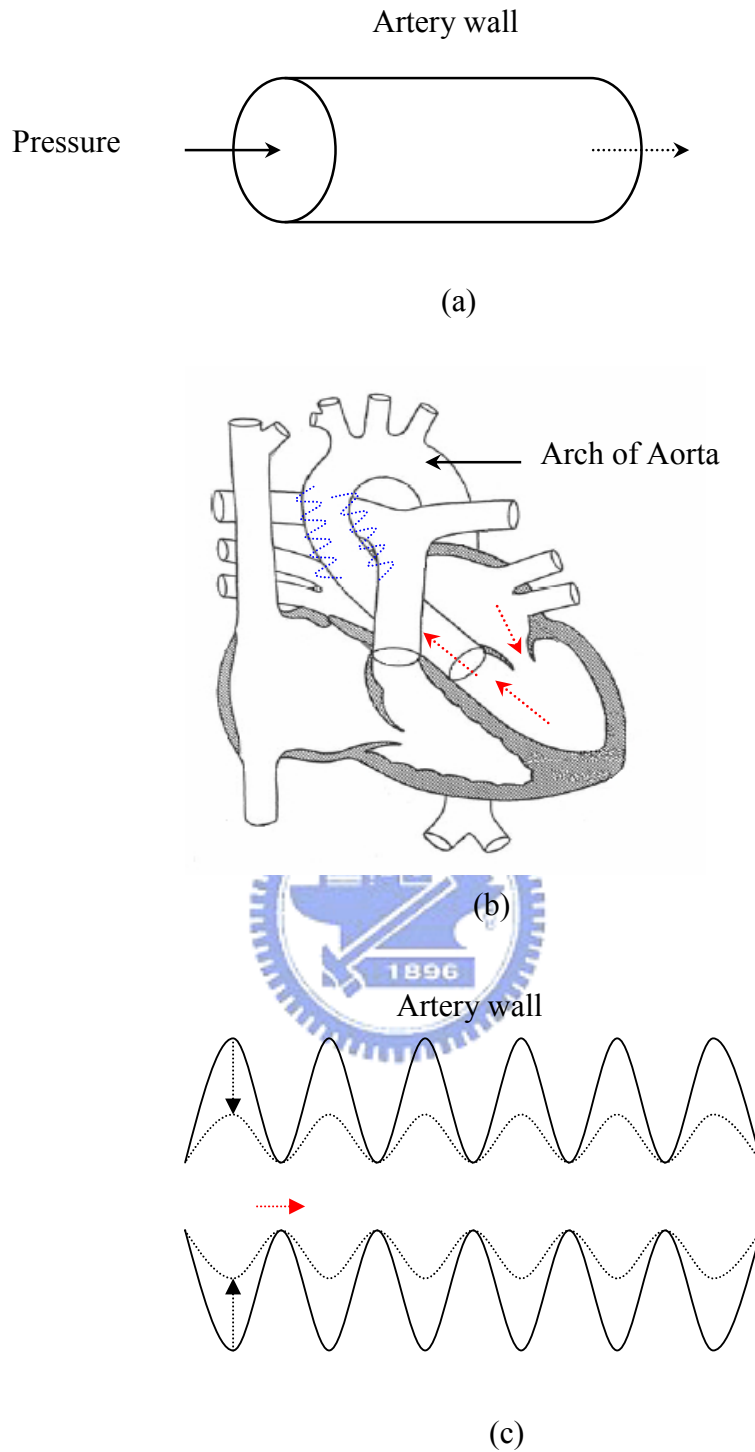
Fig. 1. (a) From the viewpoint of traditional hemodynamics, the pressure imposed on blood vessel is along the tube. (b) The 180° bending at the arch of aorta transforming the kinetic energy of blood flow into elastic potential energy of artery wall is illustrated. (c) The pressure wave resulting from the elastic potential energy propagates along the artery; thus, the wall squeezes the low blood flow forward.
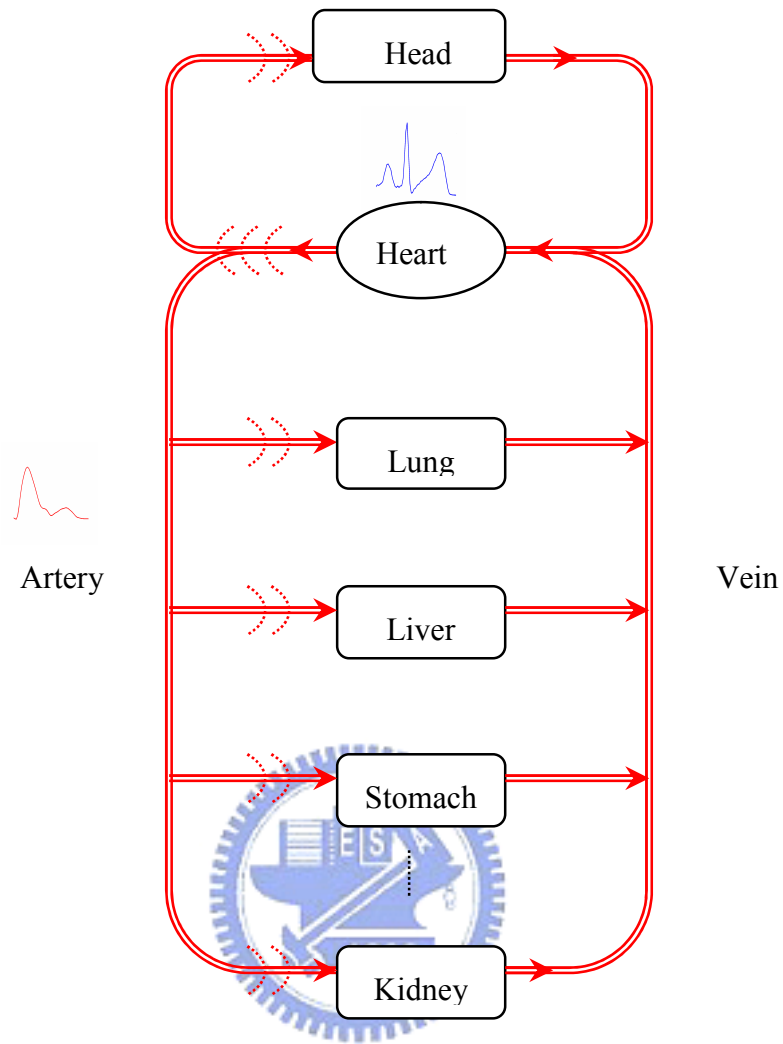
(a)
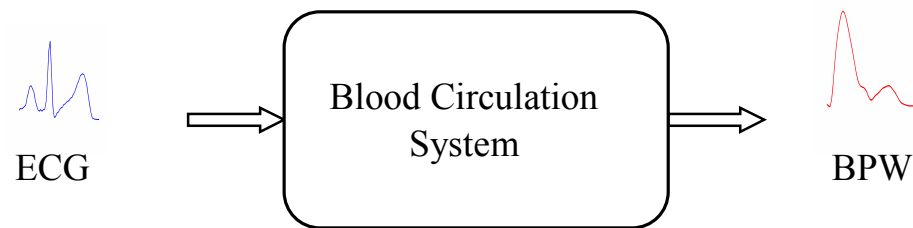
(b)

Fig. 2. (a) Schematic diagram of blood circulation system (b) The blood circulation is regarded as an electrically-driven, mechanical-pumping system.

CHAPTER 2.   RESONANCE AND COHERENCE

2.1 Concept of Resonance and Coherence

In physics, it is well known that when an object is hit or disturbed, it tends to vibrate at a particular frequency or a set of frequencies known as the natural frequency, which is associated with one of the standing wave patterns. If another interconnected object pushes it with one of the natural frequencies, it will oscillate coherently with the interconnected object and achieve the largest vibration with the least resistance. This is known as "*resonance*" [10]. Briefly, resonance exhibits the tendency of a system to absorb more oscillatory energy when the frequency of the oscillation matches the natural frequency of the vibration of the system (its resonant frequency) [3]. From the circuit viewpoint, as long as resonance occurs, the resistive elements, which will not cause frequency-dependent phase variation, are left in the circuit alone because of the cancellation between capacitive and inductive reactance [11]. Thus, the phase of output will be the same as that of input. In other words, the output will coherently oscillate with the input.

The phenomenon could be explained by a simple physical experiment demonstrated in Fig. 3. In Fig. 3, if struck by a rubber hammer, the tines of the tuning fork will vibrate back and forth and disturb the surrounding air medium; then the sound pressure wave is created. This mechanism is similar to the generation of the blood pressure wave resulting from heart beat. When the stimulated tuning fork forces air inside the first air tube with its natural frequency, which depends on the adjustment of the water level of the tube, the sound pressure wave achieves its maximum vibration, and resonance as well as coherent oscillation occur. Therefore, the maximum vibration pumps the water wave through the elastic tube and beats against the air in

the second tube. Then, a loud sound is produced. Conversely, if the tuning fork does not resonate with the first air tube, there will be no loud sound. The same theory could be applied to the heart pumping blood and blood circulation shown in Fig. 2(a).

Instead of air, blood is the medium for cardiovascular system. The heart is equivalent to the tuning fork, and the arterial system to the first air tube. In addition, because there are many arterioles distributed on organs, such as the lung, liver, heart, stomach, kidney, etc., the effect of these arterioles could be modeled as a cavity resonator similar to the second air tube. Therefore, provided that the heart resonates with the arterial system well, the organs will receive the maximum energy and coherently oscillate with the heart.

2.2 Mathematical Description

For arterial system, most of the energy originates from the transverse vibration of artery wall. The wall squeezes the blood, and via the equation of continuity of the fluid, the pressure wave drives a blood flow wave. The proposed pressure wave is governed by the following equation [4,12]

$$\mu \frac{\partial^2 P(z,t)}{\partial t^2} + R \frac{\partial P(z,t)}{\partial t} + kP(z,t) = \tau \frac{\partial^2 P(z,t)}{\partial z^2} + \frac{1}{C_A} F_{ext} \qquad (1)$$

where $P(z,t)$ is the difference between the internal fluid pressure $P_i(z,t)$ and the static pressure $P_0(z)$, i.e. $P(z,t) = P_i(z,t) - P_0(z)$, $\mu = \rho_w h + \rho_f h_f$, $k \cong \frac{E_n}{r_0} - \frac{2\pi r_0}{C_A}$,

and $\tau = E_{rz} h + T$,

in which

22

ρ_w : density of arterial wall;

h : thickness of the wall;

ρ_f : density of the fluid that adheres to the wall ;

h_f : thickness of the fluid that adhere to the wall and moves radially together with the

   wall;

R : constant of viscosity for movement of the wall and the adherent fluid in the radial

   direction;

$E_n = E_r + E_\theta$: the sum of Young's modulus in the radial and in the circumferential

   direction;

E_{rz} : the sum of Young's modulus in the shear modulus of the wall;

T : tension along the wall per-unit circumferential length;

r_0 : static radius of the tube;

C_A : arterial compliance ($= \dfrac{d(\pi r(z,t)^2)}{dP(z,t)}$);

$r(z,t)$: radius of artery.
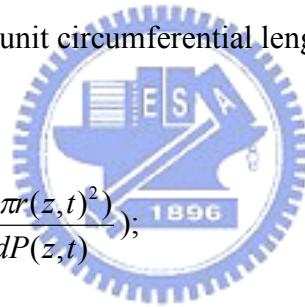
Considering the pressure in cross-section, $\dfrac{\partial^2 P(z,t)}{\partial z^2}$ will be equal to zero, and Eq. (1)

is simplified as

$$\mu \frac{\partial^2 P(t)}{\partial t^2} + R \frac{\partial P(t)}{\partial t} + kP(t) = \frac{1}{C_A} F_{ext} . \tag{2}$$

It is an equation of damped forced oscillation and can be viewed as the motion of a

spring (spring coefficient $= k$) with an inertia element (mass $= \mu$) as shown in Fig.

4(a). $P(t)$ is related to the displacement of inertia element and the viscous damping

force is proportional to the velocity (damping coefficient $= R$).

Under the assumption of electrically-driven mechanical-pumping system, F_{ext} is related to ECG. Although the real ECG signal is quasi-periodic, it can be transformed into harmonic summations by the Fourier method. Then, we can consider F_{ext} as a harmonically driving force and Eq. (2) is rewritten as

$$\mu \frac{\partial^2 P(t)}{\partial t^2} + R \frac{\partial P(t)}{\partial t} + kP(t) = \frac{F_0 \cos(wt)}{C_A} \tag{3}$$

where F_0 is the amplitude of forcing function. The particular solution of Eq. (3) is also expected to be harmonic and assumed in the following form:

$$P_p(t) = P_0 \cos(\omega t - \phi). \tag{4}$$

By substituting Eq. (4) in to Eq. (3), the amplitude (P_0) and phase angle (ϕ) of the response can be expressed as [8]

$$\frac{P_0}{\delta_{st}} = \frac{1}{\left\{ \left[1 - \left(\frac{\omega}{\omega_n} \right)^2 \right]^2 + \left[2\zeta \frac{\omega}{\omega_n} \right]^2 \right\}^{1/2}} = \frac{1}{\sqrt{(1 - r^2)^2 + (2\zeta r)^2}} \tag{5}$$

and

$$\phi = \tan^{-1} \left\{ \frac{\frac{\omega R}{\mu}}{\omega_n^2 - \omega^2} \right\}, \tag{6}$$

where

$$\omega_n = \sqrt{\frac{k}{\mu}} : \text{undamped natural frequency,}$$

$$\zeta = \frac{R}{2\mu\omega_n} : \text{damping ratio,}$$

$$\delta_{st} = \frac{F_0}{kC_A} : \text{deflection under the static force } F_0, \text{ and}$$

$$r = \frac{\omega}{\omega_n} .$$

From Eq. (5), we know that when the forcing frequency ω is equal to the undamped natural frequency (ω_n) (i.e. $r = 1$), the amplitude (P_0) becomes maximum and the condition is called *resonance*. Damping reduces the amplitude for all values of the forcing frequency and particularly at resonance. For the healthy subjects, the spectral harmonics always coincide with that of BPW, so that we can consider the spectral harmonics of BPW as the natural frequencies of arterial system [11].

For the homogeneous solution of Eq. (3), we know that if $R < 2\sqrt{\mu k}$ (i.e. less damping), the system will be under-damped and generally stay in a healthy status with better artery elasticity. The waveform of BPW in such a system is shown in Fig. 4(b), where there are three peak waves (Percussion, Tidal and Dicrotic waves). It is noted that tidal wave occurs only in someone whose elasticity of artery wall is superior. On the other hand, if $R > 2\sqrt{\mu k}$ (i.e. more damping), the system will be over-damped and has worse artery elasticity. The BPW of such a system is demonstrated in Fig. 4(c), where there is only one peak wave (Percussion wave). Clinically, the patients of arteriosclerosis often show such a waveform pattern.

2.3 Signal Acquisition

The block diagram of the instrument for detecting the BPW is shown in Fig. 5(a) and the set up diagram is demonstrated in Fig. 5(b). The ECG of lead Ⅱ and the BPW of a radial artery non-invasively detected at the wrist (Fig. 5(c)) using piezo-electric

transducer were simultaneously recorded for 15 s and digitized at a sampling rate of

100 Hz. The 3 dB frequencies of the low-pass filter are 30 Hz for BPW and 50 Hz for

ECG. The pressure detection system must consist of the pressure transducer, amplifier

circuit, and A/D circuit, all of which operate with high linearity, broad bandwidth and

fast response, to avoid distortion of the pulse waveform. Then we can obtain an

accurate spectral distribution.
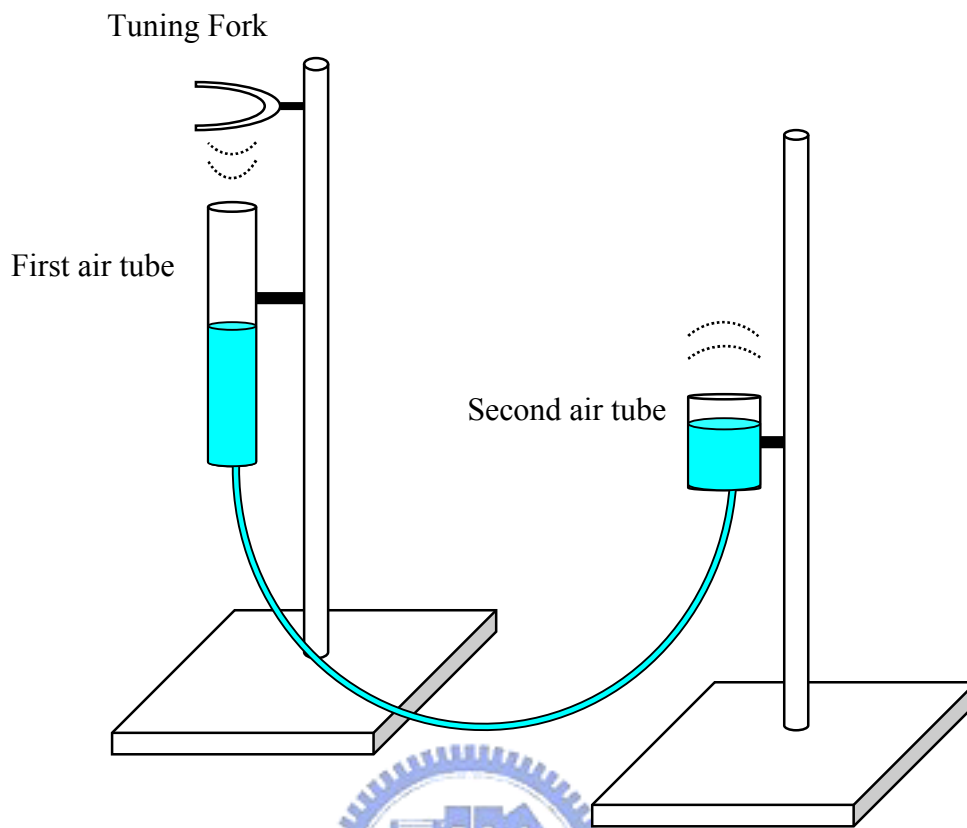
Fig. 3. If the stimulation frequency of tuning fork is equal to the natural frequency of the first air tube, the tuning fork resonates with the first air tube; thus, the maximum sound pressure wave of output is produced in the second air tube.

(a)

Percussion wave

Tidal wave

Dicrotic wave

(b)

Percussion wave

(c)
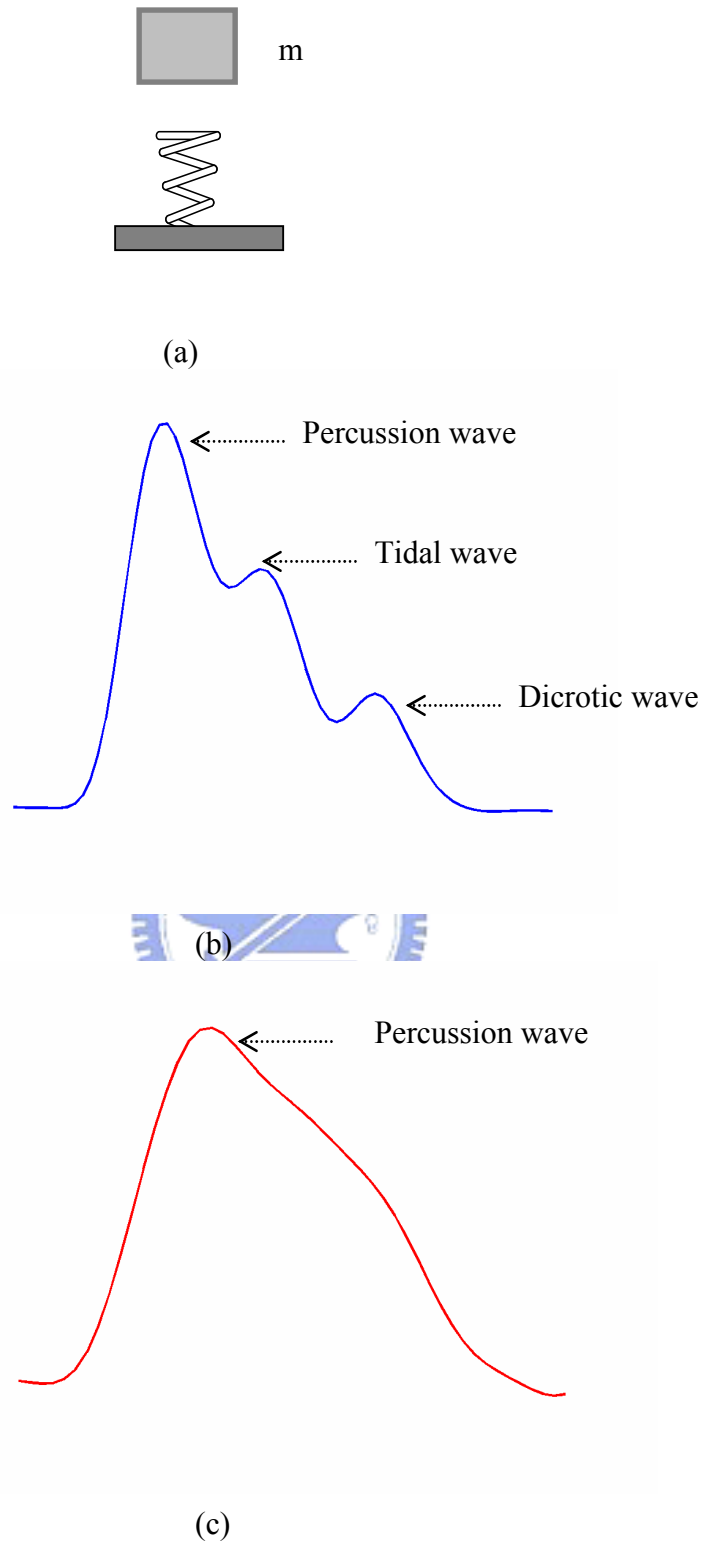
Fig. 4. (a) The vibration of artery behaves like the motion of a spring with mass m. (b) The under-damped BPW waveform with three peaks (Percussion, Tidal and Dicrotic waves) is shown. (c) The over-damped BPW waveform with single peak (Percussion wave) is illustrated.
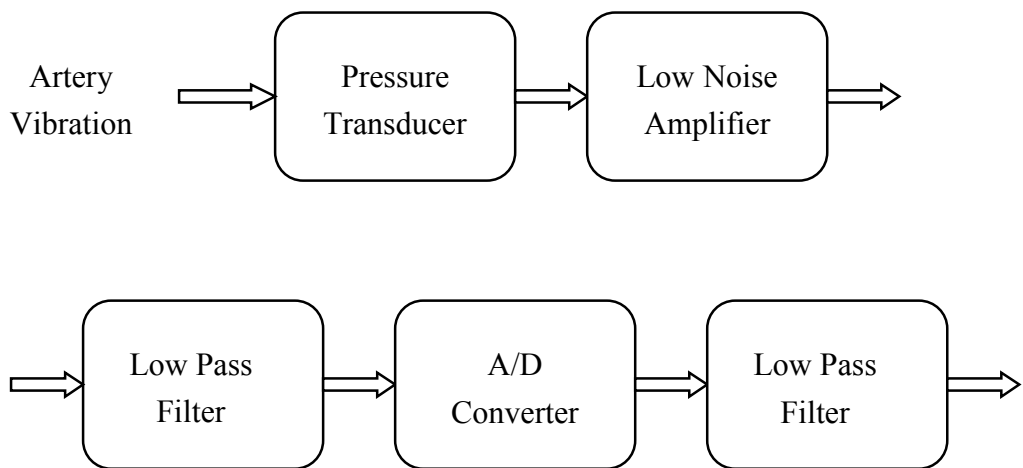
(a)
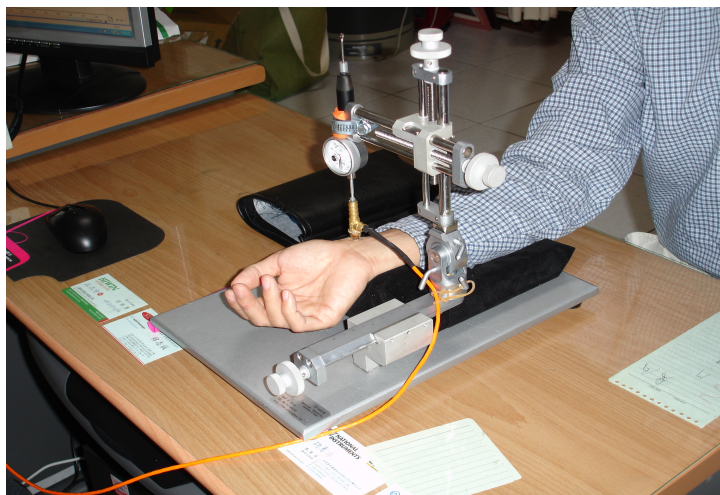
(b)

(c)
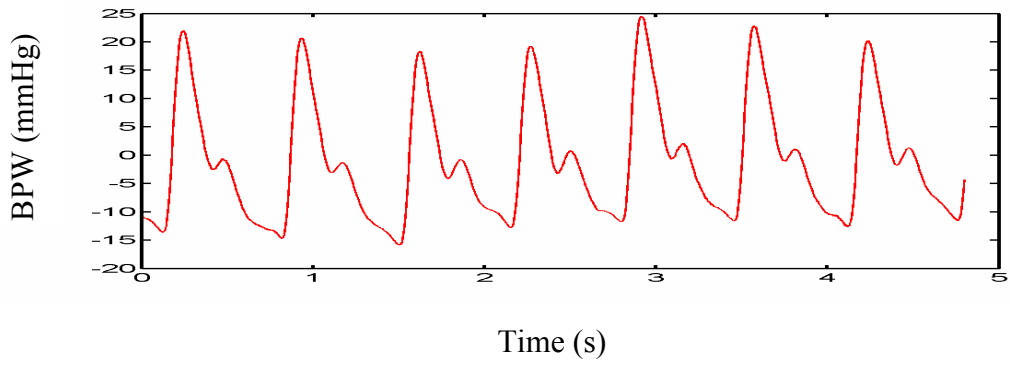
(d)
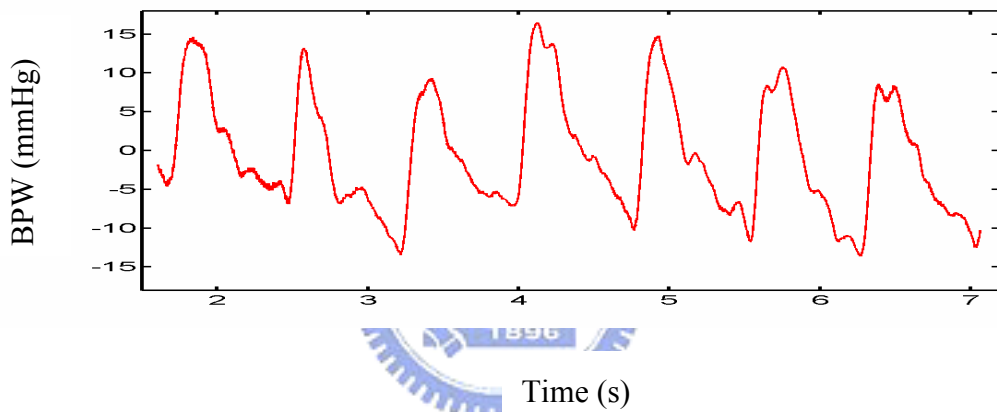
(e)
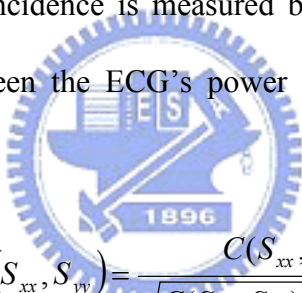
Fig. 5 (a) The block diagram of the BPW detection instrument is illustrated. (b)The set up diagram of BPW detection instrument is shown. (c) The detection point at artery is shown. (d) A BPW of normal person is shown. (e) A BPW of patient is shown.

CHAPTER 3. SPECTRAL-DOMAIN ANALYSIS

3.1 Power Spectrum Analysis

To investigate the different characteristics of the blood circulation system between two groups, a number of parameters were evaluated mainly using the frequency-domain methods. First, Fourier analysis was applied to characterize the quality of the BPW coupled with heart pumping (ECG). The power spectral density (power spectrum) was estimated from the averaged periodogram, i.e., Welch's method, using a 500-sample window with an overlap of 400 samples.

The degree of spectral coincidence is measured by the correlation coefficient or coupling efficiency (ρ) between the ECG's power spectrum (S_{xx}) and the BPW's power spectrum (S_{yy}); that is,

$$\rho\left(S_{xx},S_{yy}\right)=\frac{C(S_{xx},S_{yy})}{\sqrt{C(S_{xx},S_{xx})C(S_{yy},S_{yy})}}, \qquad (7)$$

where $C(S_{xx},S_{xx})$ is the auto-covariance of the power spectral density, S_{xx}, and $C(S_{xx},S_{yy})$ is the cross-covariance of power spectral densities S_{xx} and S_{yy} [13].

Figure 6 displays the power spectra (in dB scale) of the ECG and BPW for one normal, healthy subject (Fig. 6(a)) and one vascular patient (Fig. 6(b)). The spectral magnitudes of both the ECG and BPW are normalized to the same value according to the peak magnitude at the fundamental frequency, which is about 1.1 Hz for the healthy subject and 1.0 Hz for the patient. Apparently, the spectra of the ECG and BPW for the healthy subject coincide well for frequencies below 6 Hz, over which range more than 90% of the power is distributed. The correlation coefficient between

the ECG and the BPW estimated by Eq. (7) is approximately 0.98 in the frequency band from 0 to 20 Hz for the healthy subject. When most parts of the BPW's power spectrum coincide with those of the ECG, that is, when the spectrum is coupled from the ECG to the BPW, we call this phenomenon the *spectrum-coupled effect*, which is similar to the *frequency matching* effect resulting from resonance. However, the spectra for the patient deviate widely except for the fundamental frequency. The correlation coefficient estimated by Eq. (7) is approximately 0.24. This suggests that the input-to-output (I/O) spectral relation is highly uncorrelated or out of resonance for abnormal blood circulation.

3.2 Bispectrum Analysis

As long as resonance occurs in an RLC circuit, the driving signal keeps the same phase as the output signal due to the cancellation of inductive and capacitive effects. Thus, to further investigate the *phase-coupled effect* between the ECG and the BPW, we evaluated the cross-bicoherence parameter on the basis of the bispectral analysis approach since the second-order spectrum (power spectrum) analysis disregarded the phase relations between frequency components [14,15]. The bispectrum $B(f_1, f_2)$ of a signal with Fourier transform $X(f)$ is defined as: $B(f_1, f_2) = X(f_1) X(f_2) X^*(f_1+f_2)$. Huber et al. used the bispectrum to investigate the EEG phase relation [16]. Jamesek et al. computed the cross-bispectrum between ECG and respiratory signals to study the coupling between cardiac and respiratory activities [17]. One major advantage of the bispectral approach is its ability to detect quadratic phase coupling. The interaction between two harmonic components of a process results in considerable spectral activities at the sum and difference of the two frequencies. It is the so-called

quadratic phase coupling, and it arises only among harmonically related components. In practical applications, bicoherence defined as follows provides a normalized expression with a small variance:

$$bic(f_1, f_2) = \frac{|B(f_1, f_2)|^2}{P(f_1)P(f_2)P(f_1 + f_2)}, \qquad (8)$$

where $B(f_1, f_2)$ is the estimate of the bispectrum, and $P(f)$ is the estimate of the power spectrum. The values of bicoherence lie between 0 and 1, with 0 (1) indicating the lowest (highest) degree of coupling [18,19].

In order to investigate the input-output relation, a cross-bispectrum is used to quantify the cross quadratic phase coupling, which is defined as $B_{WXY}(f_1, f_2) = W(f_1)X(f_2)Y^*(f_1 + f_2)$, where $W(f_1)$, $X(f_2)$ and $Y(f_1 + f_2)$ denote the Fourier transform of three signals, W, X, and Y. Accordingly, the cross-bicoherence can be evaluated as follows

$$bicx(f_1, f_2) = \frac{|B_{WXY}(f_1, f_2)|^2}{P_W(f_1)P_X(f_2)P_Y(f_1 + f_2)}. \qquad (9)$$

For $B_{WXY}(f_1, f_2)$, a peak at the location (f_1, f_2) indicates that the frequency component $(f_1 + f_2)$ of Y is generated due to the quadratic phase coupling effect contributed by the f_1 component in W and the f_2 component in X. In our research, W is assumed to be the ECG signal, and X and Y are assumed to be the BPW [14,15]. In this study, we computed the average of cross-bicoherence values at significant frequency coordinates to measure the degree of cross quadratic phase coupling from

the ECG (input) to the BPW (output).

As illustrated in Fig. 7, ECG bicoherence plots for the normal and vascular subjects (the top row) both reveal a landscape of recurrent peaks at coordinates (f_0, f_0), $(2f_0, f_0)$, …, and $(f_0, 4f_0)$, where f_0 is the fundamental heartbeat frequency. However, considerable distinction between both subjects was observed in BPW bicoherence plots (the mid row). The BPW bicoherence for the patient shows an irregular distribution of peaks and a much weaker quadratic-phase coupling resulting from the poor resonant behavior of the cardiovascular system. In the healthy subject, the cross-bicoherence (the bottom row, Fig. 7(a) is characterized by an orderly alignment and robust peaks of magnitude ≥ 0.7 at coordinates (mf_0, nf_0), $1 \leq m, n \leq 4$. The average value of cross-bicoherence measured at these frequency pairs is about 0.92. This implies that a strong cross quadratic-phase coupling between ECG and BPW is present at these low frequencies constituting the majority of the signal power. This also suggests that the "phase dependence" between input and output of the system is coupled. In comtrast, the average of the cross-bicoherence analyzed for the patient is about 0.59, with highly irregular shape, in the frequency range defined. Consequently, the bicoherence analysis infers a weaker cross quadratic-phase coupling between ECG and BPW for a diseased circulatory system.

3.3 Transfer Function Analysis

Finally, the frequency response of the circulation system model, under the assumption of linearity and time-invariance (LTI), can be expressed as the ratio

$$H(f) = \frac{P_{XY}(f)}{P_{XX}(f)}, \tag{10}$$

where P_{XX}(f) and P_{XY}(f) represent the auto power spectrum of the input and the cross power spectrum of the input and output [13]. The units used for ECG and BPW in the evaluation are μV and mmHg, respectively. The function $H(\cdot)$ denotes a transfer function corresponding to the "input-to-output transfer gain" measurement and reflecting the linear relation between ECG and BPW.

Figure 8 illustrates the magnitude of transfer function $H(f)$ estimated by Eq. (10) and normalized by the mean value, based on a 500-sample Kaiser window and 400 points overlapped. Apparently, the response in Fig. 8 of this normal subject approximates a constant at frequencies below 6 Hz. This kind of flat response characterizes an LTI system with smooth energy transfer and low resistance. Thus, it is considered to be a system with good transmission efficiency from input to output in the corresponding frequency range. Nevertheless, the response for the patient in Fig. 8 exhibits severe fluctuation, indicating poor transmission efficiency or high resistance from input to output. The standard deviation of $H(f)$ in the range 0-10 Hz is used to measure the system performance in frequency domain, which is 0.19 and 0.36, respectively, for the normal and abnormal subjects.

3.4 Experiment and Results

The study subjects were composed of two groups. The first group consisted of 20 subjects (11 males and 9 females, at the ages of 18 to 40) whose health checks were normal. The second group was composed of vascular patients (12 males and 8 females, at the ages of 36 to 55), among whom eight subjects had hypertension; seven subjects, atherosclerosis; and the rest, thrombus diseases. Before measurement, all subjects rested for about twenty minutes to obtain a steady pulse, because a changing heart rate,

e.g. because of physical exercise, leads to blood redistribution and yields an unreliable result. Although there are many possible reasons for changes in the natural frequency of the arterial system that result in the vessel or organ diseases, we confined our preliminary study to vascular-related diseases, such as hypertension, atherosclerosis, and thrombus diseases.

Table 1 summarizes the results from 20 healthy subjects and 20 vascular patients, including the correlation coefficient of power spectrum (0-20 Hz), the average of the cross-bicoherence ((mf_0, nf_0), $1 \leq m, n \leq 4$), the standard deviation of the transfer function (0-10 Hz), and the p-value. In the group of healthy subjects, larger mean values of correlation coefficient and cross-bicoherence are derived from the distributions; however, a smaller mean value of transfer function deviation is obtained. Moreover, all p-values are lower than 0.01. We may thus declare that the difference between two groups is significant on the basis of the evaluation of these parameters.

To evaluate the distribution of data set of each group, the results are embedded in the three dimensional feature spaces: (correlation coefficient, the standard deviation of transfer function, cross-bicoherence), as displayed in Fig. 9. Two distinct clusters of feature vectors are formed corresponding to the normal and abnormal groups.

3.5 Spectral-Domain Circuit Model

Some researchers discussed that most of the energy in blood circulation is transported by the transverse vibration of arterial walls. This mechanism makes *transverse resonance* possible, although resonance along the longitudinal artery was supposed to have failed according to McDonald [2]. In fact, the effect of transverse resonance has been found in electromagnetic waves propagating along a planar-plate

waveguide [20]. Because of zero impedance in the transverse direction (transverse resonance), the energy can be preserved in transverse direction; thus, the blood pressure wave can be carried a distance in the longitudinal direction. In the electromagnetic waveguide theory, different resonance modes correspond to the respective frequencies in the spectrum. Therefore, in order to survey the resonance effect in blood circulation, we have analyze and established a spectral-domain circuit model of the arterial system.

Starting from the conventional time-domain Windkessel model (Fig. 10(a)) which is used to represent the whole arterial system, the compliance (C) and inertance (L) are closely related to the capacitance and inductance in an electrical circuit, respectively [1,2]. Resistance R_1 is connected in serial with L, and peripheral resistance R_2 is connected in parallel with C. By circuit theory, one pair of capacitance and inductance generates only a single resonance frequency (i.e., a single peak frequency in the spectrum). The phenomenon is against the real spectrum of BPW, in which multiple resonance frequencies are observed. Therefore, we must make some modifications of the conventional Windkessel model to match the frequency-domain characteristics. The original Windkessel model with four elements is assumed to be a single resonator unit. This resonator is reproduced into five units, which are connected in parallel to simulate five major resonance frequencies constituting most of the energy of the BPW. If any other frequencies are indispensable, resonance units can be extended and connected in parallel. In addition, the resonance frequency of each resonator unit is assumed to be sufficiently separated so that it does not cause inter-coupling between resonators. In fact, almost all observed peaks in the power spectrum are discrete enough to support this assumption.

The new spectral-domain circuit model is plotted in Fig. 10(b). The resonance

frequency f_0 and the resonance quality factor (Q) may be derived as follows. First, the parallel circuit of R_2 and C in Fig. 10(a) is transformed into the serial $R_2^{'}$ and C' in Fig. 10(c). Then C' and $R_2^{'}$ can be derived as

$$C^{'} = C + \frac{1}{\omega^2 R_2^{\ 2} C} \tag{11}$$

$$R_2^{'} = \frac{R_2}{1 + \omega^2 R_2^{\ 2} C^2}, \tag{12}$$

where ω is the angular frequency. When the imaginary part of the input impedance of RLC serial circuit becomes zero, resonance occurs, and the resonance frequency is given by

$$f_0 = \frac{1}{2\pi} \sqrt{\frac{R_2^{\ 2} C - L}{R_2^{\ 2} C^2 L}}. \tag{13}$$

Bandwidth (BW), defined as the frequency range between 3 dB points in the power spectrum, is derived as

$$BW = \frac{1}{2\pi} \sqrt{\left(\frac{R_1 + R_2^{'}}{L}\right)^2 + \frac{4}{LC^{'}}}. \tag{14}$$

According to the theory of resonance circuits, the loaded Q of the Windkessel resonator with a narrow band, which is defined as the total stored energy (E_S) divided by the total energy loss (E_L), may be approximated from Eqs. (13) and (14) as

$$Q \equiv \frac{E_S}{E_L} = \frac{f_0}{BW}, \tag{15}$$

where f_0 is the resonance frequency and BW is the 3 dB bandwidth of the power spectrum [20]. Instead of calculating the parameters R_1, R_2, L, and C of the model to obtain f_0, BW ,and Q, we measured f_0 and BW directly from the real spectrum to

evaluate Q. In fact, once f_0 is known from the spectrum, the relationship between L and C can be determined by Eq. (13). In the same manner, if BW is measured from the spectrum, the derivation of R_1 and R_2 depends on BW in Eq. (14). Therefore, f_0, BW, and Q are sufficient to characterize the model, and it is not necessarily essential to evaluate R_1, R_2, L, and C. As a result, we obtain the quality of an individual resonator from its corresponding resonance band in the real spectrum.

In summary, in the traditional Windkessel model with four elements, the overall compliance and inertance effects are merged and degenerated, respectively; therefore, to remain consistent with the practical spectrum, we decompose the traditional model into multiple resonance units with different resonant frequencies. The decomposed model is similar to the topology of blood circulation within the human body, where the heart pumps the blood to several major organs such as the liver, heart, spleen, lungs, and kidneys. Every organ can be considered to be connected in parallel with the aorta and behaves like a group of arterioles. From the viewpoint of a circuit, the organ also looks like a band-pass filter or a resonator which resonates with the heart [6].

In order to simulate the frequency response of the spectral-domain circuit model, we put in an AC current source with 1A amplitude to simulate blood flow. It is worth noting that the relation between blood flow and arterial pressure is assumed to be linear. To design the resonance frequencies of the model to match the real spectrum with 1 Hz fundamental frequency, by Eq. (13) we let $L_1 = 0.16\,(\text{H})$, $C_1 = 0.16\,(\text{F})$, $L_2 = 0.08$ (H), $C_2 = 0.08$ (F), $L_3 = 0.053$ (H), $C_3 = 0.053$ (F), $L_4 = 0.04$ (H), $C_4 = 0.04\,(\text{F})$, $L_5 = 0.032\,(\text{H})$, $C_5 = 0.032\,(\text{F})$, the serial resistances (R_{11}, R_{21}, R_{31}, R_{41}, and R_{51}) be zero, and the parallel resistances (R_{12}, R_{22}, R_{32}, R_{42}, and R_{52}) be 10k (Ω) in the circuit of Fig. 10(b). Thus, the resonators operate with resonance

frequencies of approximate 1, 2, 3, 4, and 5 Hz, i.e., f, $2f$, $3f$, $4f$, and $5f$, respectively, where f is the beat frequency. The simulated frequency response from SPICE program is shown in Fig. 11(a). Note that increasing the serial resistances (R_{11}, R_{21}, R_{31}, R_{41}, and R_{51}) decreases the amount of current flowing into the resonators, gradually broadening the resonance frequency band, and decreasing the Q value. This statement is illustrated in Fig. 11(b). Moreover, in Fig. 11(c) the decreasing parallel peripheral resistances (R_{12}, R_{22}, R_{32}, R_{42} and R_{52}) reveal similar results as in Fig. 11(b). These results also indicate that only some specific resonance frequencies, which are integral harmonics of the fundamental heart frequency, are allowed to pass the arterial system. This agrees with the fact that the arterial system not only couples the energy from the heart but also merely resonates in the corresponding harmonic frequencies. Consequently, the proposed spectral-domain circuit model is well-suited for modeling the frequency behavior of blood circulation on the basis of resonance.

The equivalent resonance circuit (spectral-domain circuit model) is only used to describe the frequency matching effect (resonance) between the ECG and the BPW at several major harmonic frequencies, $f_0, 2f_0, \cdots 5f_0$, where f_0 is the fundamental heartbeat frequency. The sub-harmonic frequencies observed in Fig. 6(a) are caused mainly by the modulation effect of respiratory activity on the ECG, which then leads to a similar frequency variation in the BPW. Therefore, for healthy subjects with elastic artery walls, we observe a similar spectral distribution not only at major harmonics but also at sub-harmonics. Consequently, the transfer function is constant in the spectrum, yet there are several peaks in the simulated frequency response of the equivalent resonance circuit.

3.6 Measurement of Q Value

Taking as an example the spectra shown in Fig. 6, we observe that the frequency peaks of a patient are widen compared with those of a healthy subject. The Q values of the first five harmonics are evaluated using Eq. (15) and listed in Table 2. The result suggests that a healthy subject retains a higher Q value and a better resonance quality. Table 3 shows the statistical results of Q values for forty subjects reported in § 3.4. The higher mean Q in the healthy group further supports our conclusions in Table 2. Furthermore, the smaller P values (< 0.01) for five peak frequencies also indicate that the distinction between the two groups is significant and more obvious for higher-frequency peaks.
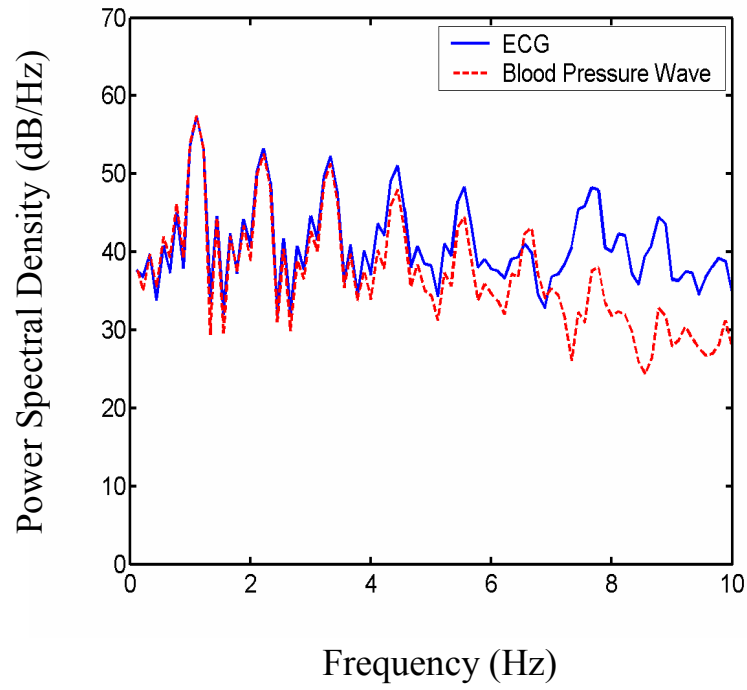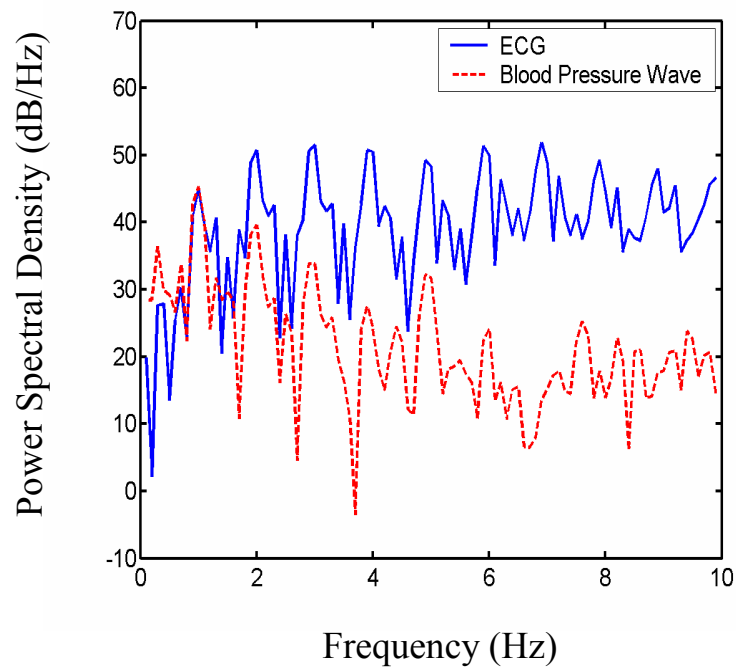
Fig. 6. Power spectral densities of ECG (solid curve) and BPW (dashed curve) for (a) a healthy subject, and (b) a cardiovascular-related patient.

ECG

ECG

BPW

BPW
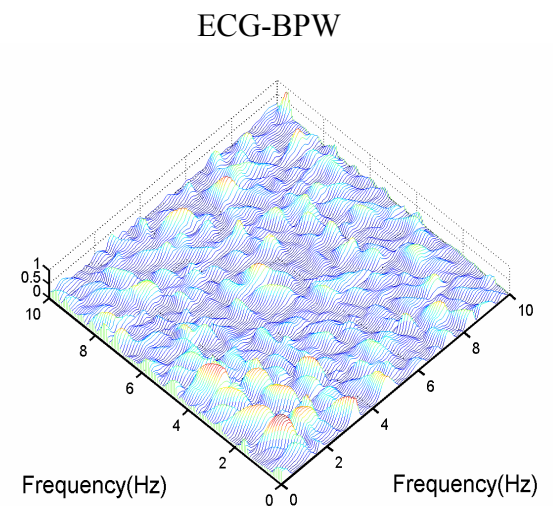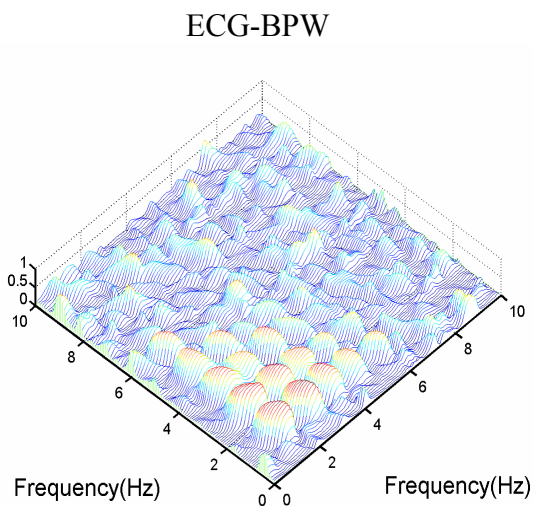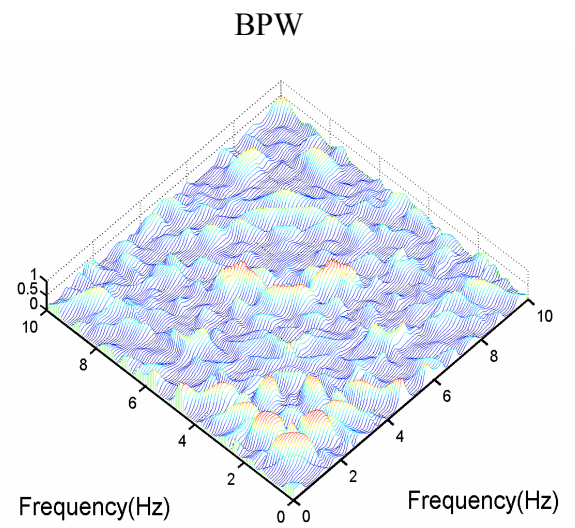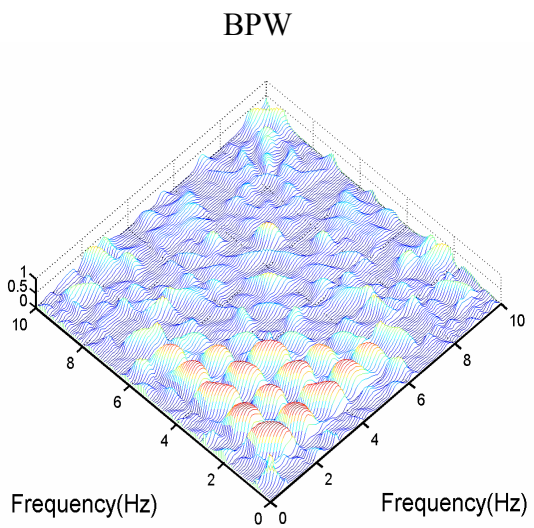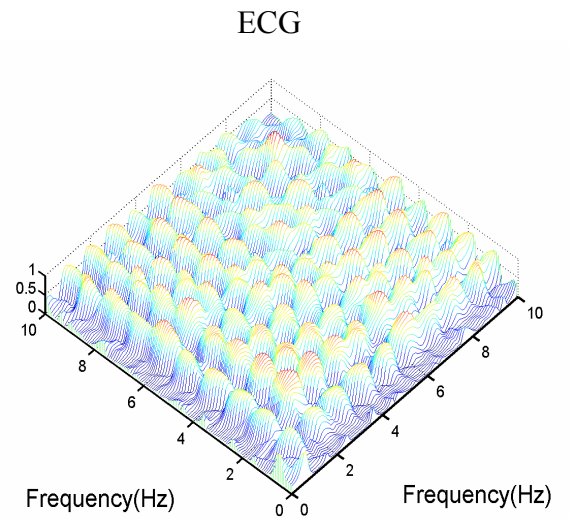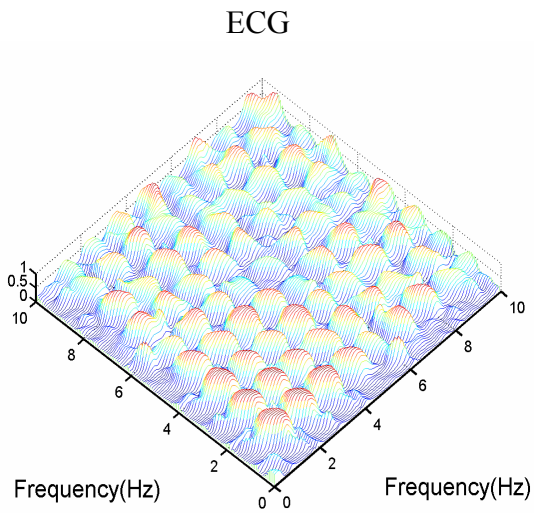
ECG-BPW

ECG-BPW

(a)

(b)

Fig. 7. ECG bicoherence, BPW bicoherence, and ECG-BPW cross-bicoherence of (a) the healthy subject, and (b) the patient.
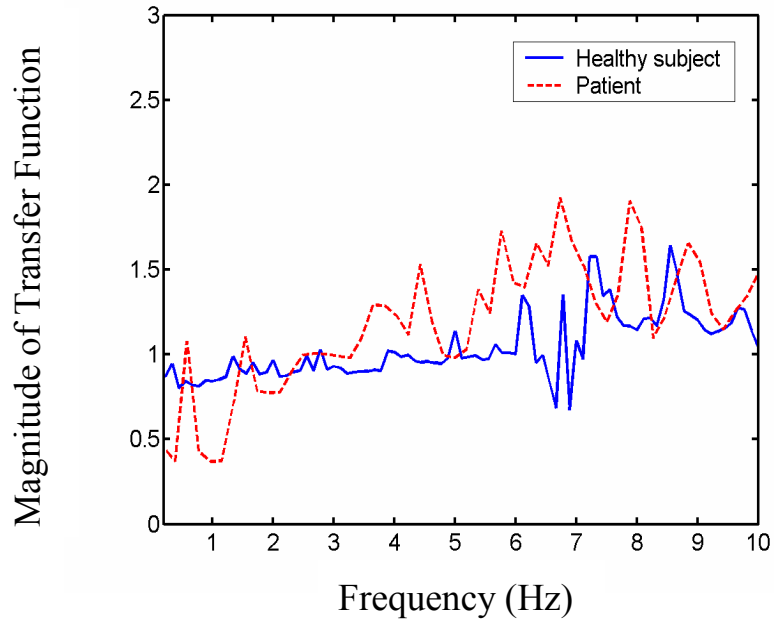
Fig. 8. Estimated transfer function of the healthy subject (solid curve) and the patient (dashed curve).
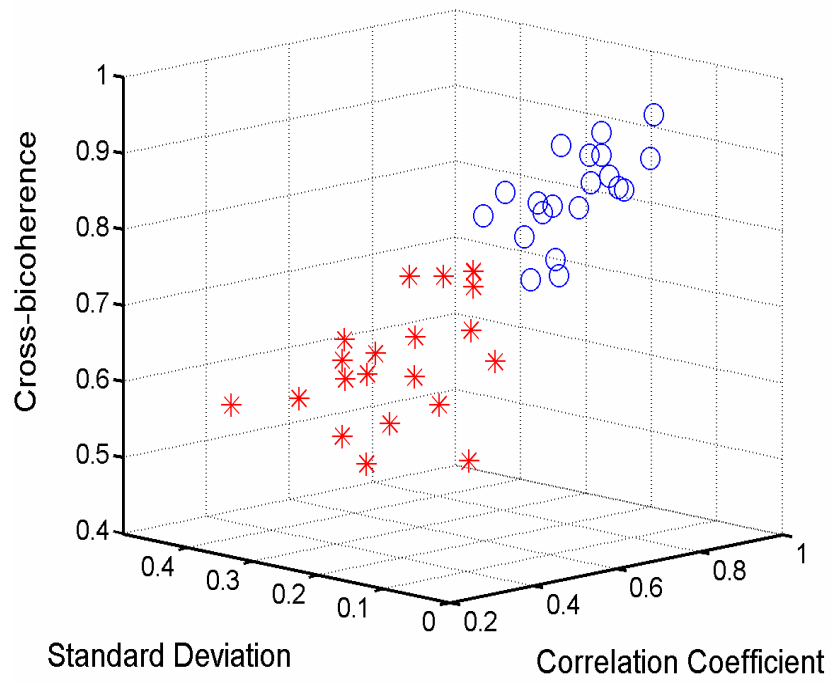
Fig. 9. The results of analyzing twenty healthy subjects and twenty vascular patients are embedded in the three dimensional feature spaces: (correlation coefficient, the standard deviation of transfer function, and cross-bicoherence). Circles (○) represent the healthy subjects and asterisks (✳) represent the patients.

(a)

(b)

(c)
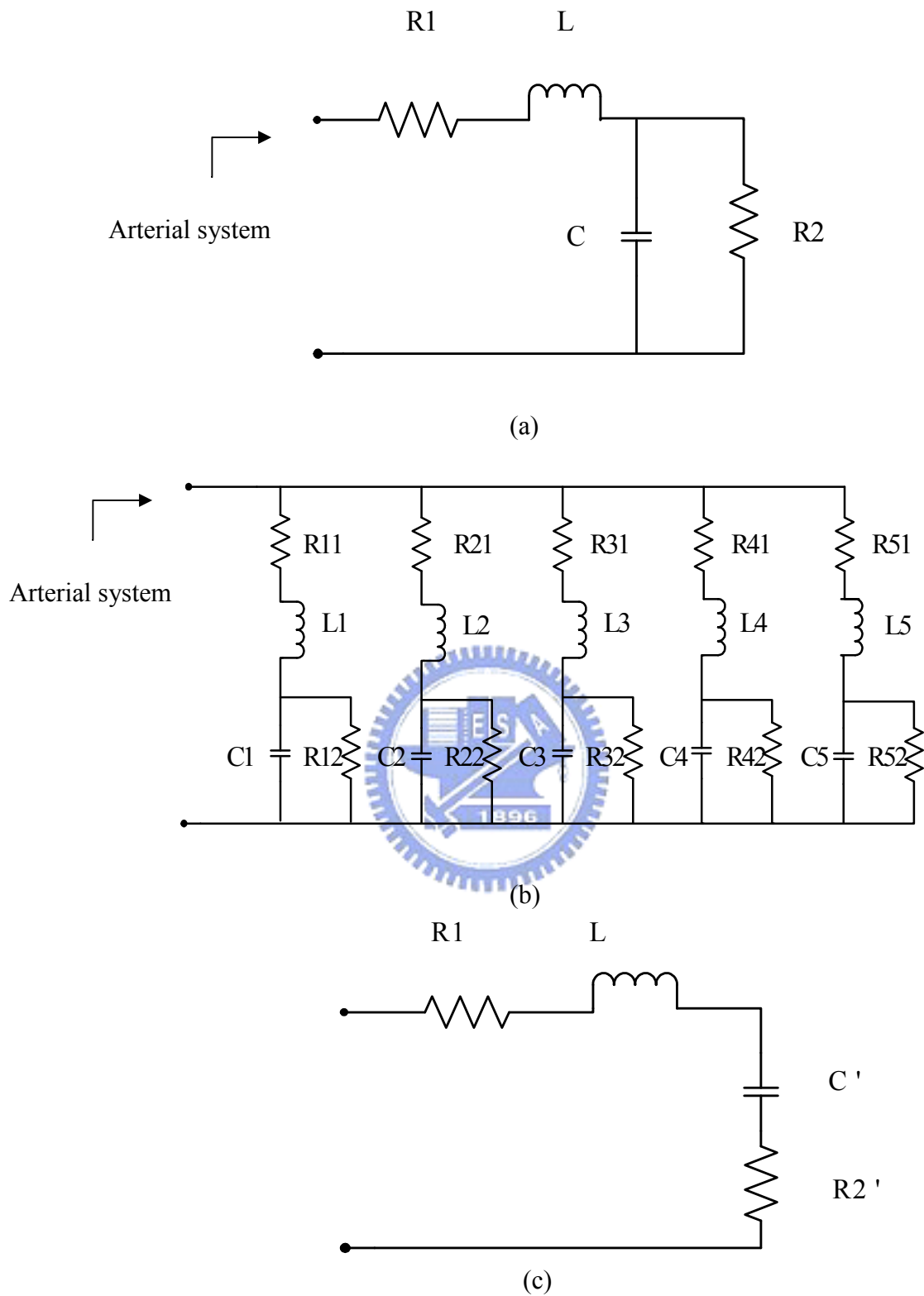
Fig. 10. (a) The Windkessel model with four elements, (b) The spectral-domain circuit model, and (c) the serial equivalent circuit of Windkessel model with four elements are illustrated.
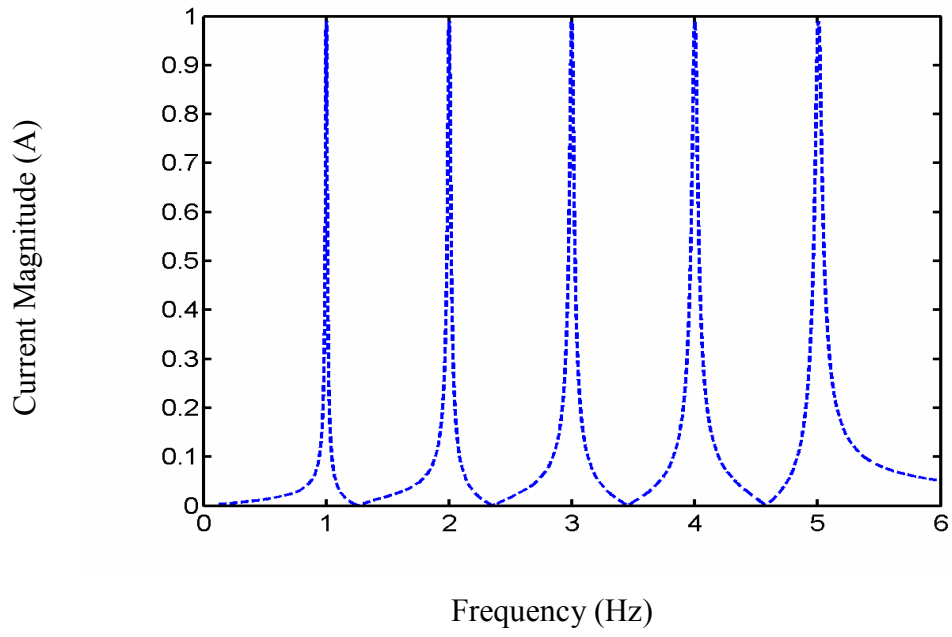
(a)
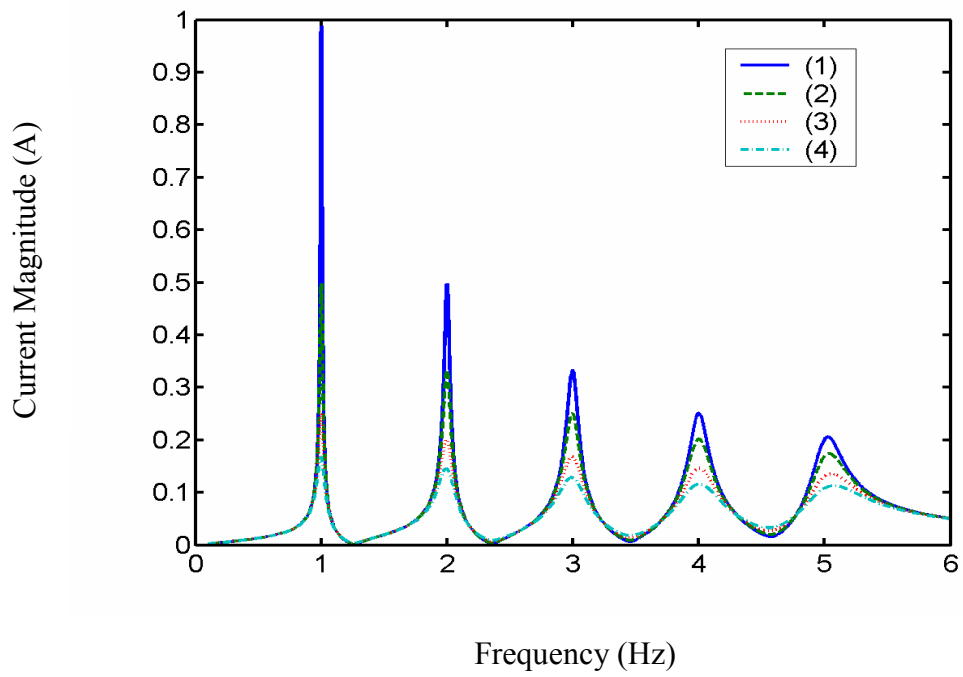
(b)
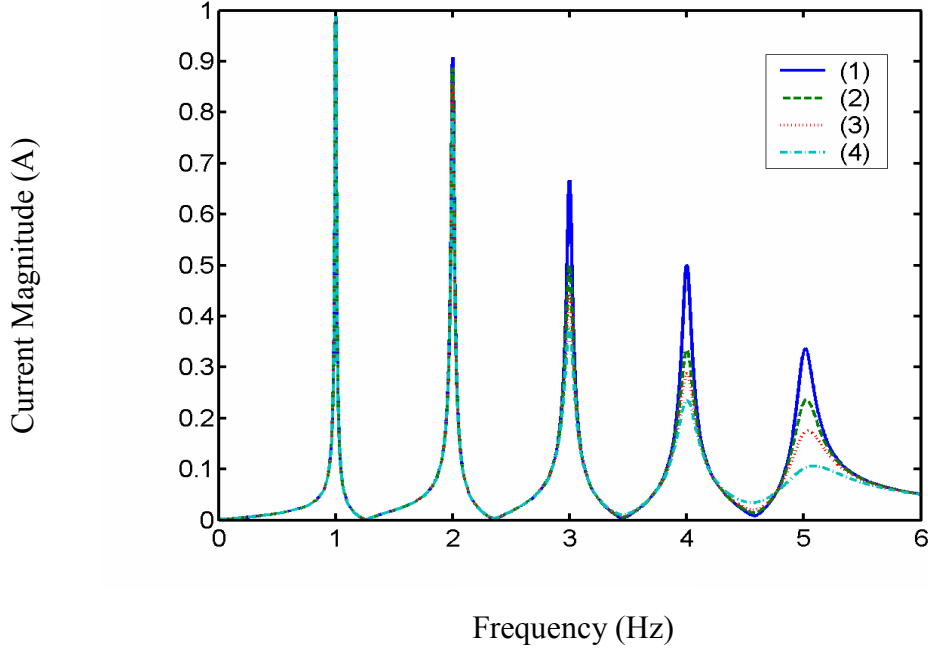
(c)

Fig. 11. The frequency response of the spectral-domain circuit model is simulated using various parameters to assess the resonance characteristics. (a) $R_{11} = R_{21} = R_{31} = R_{41} = R_{51} = 0$ and $R_{12} = R_{22} = R_{32} = R_{42} = R_{52} = 10k$ (Ω), (b) curve 1: $R_{11} = 0$, $R_{21} = 0.01$, $R_{31} = 0.02$, $R_{41} = 0.03$, $R_{51} = 0.04$ (Ω), curve 2: $R_{11} = 0.01$, $R_{21} = 0.02$, $R_{31} = 0.03$, $R_{41} = 0.04$, $R_{51} = 0.05$ (Ω), curve 3: $R_{11} = 0.03$, $R_{21} = 0.04$, $R_{31} = 0.05$, $R_{41} = 0.06$, $R_{51} = 0.07$ (Ω), curve 4: $R_{11} = 0.05$, $R_{21} = 0.06$, $R_{31} = 0.07$, $R_{41} = 0.08$, $R_{51} = 0.09$ (Ω), and $R_{12} = R_{22} = R_{32} = R_{42} = R_{52} = 10k$ (Ω) for all curves, (c) curve 1: $R_{12} = 10k$, $R_{22} = 1k$, $R_{12} = 0.2k$, $R_{12} = 0.1k$, $R_{12} = 50$ (Ω), curve 2: $R_{12} = 10k$, $R_{22} = 0.8k$, $R_{12} = 0.1k$, $R_{12} = 50$, $R_{12} = 30$ (Ω), curve 3: $R_{12} = 10k$, $R_{22} = 0.6k$, $R_{12} = 80$, $R_{12} = 40$, $R_{12} = 20$ (Ω), curve 4: $R_{12} = 10k$, $R_{22} = 0.4k$, $R_{12} = 60$, $R_{12} = 30$, $R_{12} = 10$ (Ω), and $R_{11} = R_{21} = R_{31} = R_{41} = R_{51} = 0$ for all curves.

Table 1. Statistical characteristics of correlation coefficient, cross-bicoherence, standard deviation (S.D.) of transfer function, and p-value for healthy and patient groups.

	Correlation coefficient	Cross-bicoherence	Standard deviation of transfer function
Healthy subjects (Mean ± S.D.)	0.821 ± 0.100	0.828 ± 0.056	0.206 ± 0.035
Vascular patients (Mean ± S.D.)	0.542 ± 0.110	0.619 ± 0.075	0.301 ± 0.054
p-Value	3.742×10^{-10} (< 0.01)	6.570×10^{-13} (< 0.01)	8.661×10^{-8} (< 0.01)

Table 2. Resonance quality factors (Q) of subjects shown in Fig. 6

Resonance frequency	f	$2f$	$3f$	$4f$	$5f$
Healthy subject	5.5	11.1	16.5	22.3	28.1
Vascular patient	5.3	8.0	10.5	11.1	22.3

Table 3. Statistical results for resonance quality factor (Q) of 20 healthy subjects and 20 vascular patients

Resonance frequency	f	$2f$	$3f$	$4f$	$5f$
Healthy subjects (Mean ± S.D.)	5.68±0.39	10.59±0.81	15.45±0.82	20.65±1.65	27.35±1.61
Vascular patients (Mean ± S.D.)	5.38±0.14	9.77±0.75	13.99±1.67	18.19±2.47	24.19±2.31
p-Value	2.17×10^{-3} (< 0.01)	1.93×10^{-3} (< 0.01)	1.21×10^{-3} (< 0.01)	6.74×10^{-4} (< 0.01)	1.24×10^{-5} (< 0.01)

CHAPTER 4. SYSTEM MODEL

4.1 Modulated ECG

Several influence factors, such as respiratory activity, autonomic nervous system, baroreceptor reflex, cardiac output, emotions, exercise, etc. are known to affect both the frequency and amplitude of ECG. Since ECG and influence factors are similar to a carrier and modulation signals, respectively, both the frequency and amplitude variations of ECG are essentially analogous to the frequency modulation (FM) and amplitude modulation (AM) effects in an electronic communication system.

Regarding AM effect, it is mainly caused by the respiration-induced amplitude modulation of ECG [21,22]. By the modulation theory of electronic communication we know that if the central frequency of carrier (original ECG) and AM modulation signal are f_0 and f_1, respectively, the nonlinear *inter-modulation* effect between carrier and AM modulation signal will lead to the frequency peaks at $f_0 - f_1$, $f_0 + f_1$, $f_0 - 2f_1$, $f_0 + 2f_1$, …… etc. in the spectrum [23]. Consequently, there will be some frequency components in the spectrum like harmonics, f_0, $2f_0$, $3f_0$,…,f_1, $2f_1$, $3f_1$,…, $f_0 - f_1$, $f_0 + f_1$, $f_0 - 2f_1$, $f_0 + 2f_1$, …… etc. Furthermore, because of the spectral coupling effect, there will be a similar spectrum distribution for blood pressure wave [11]. For example, for a subject whose fundamental heart beat and respiratory frequency are 1.1 and 0.3 Hz, respectively, we could find the side peaks at 0.8 Hz (1.1-0.3) and 1.4 Hz (1.1+0.3) around the first harmonic (1.1 Hz), respectively as shown in Fig. 12(a). The strength of AM modulation is called the depth of modulation and defined as follows:

$$\text{AM modulation depth} = \frac{A - B}{A + B}, \tag{16}$$

where A and B is the maximum and minimum peak amplitude of QRS complex wave of modulated ECG [23]. The ECG of this subject is demonstrated in Fig. 12(b) and the dash line denotes the amplitude variation of the peaks of QRS complex wave. Using Eq. (16), the evaluated AM modulation depth is 3.27% (A=1.025 mV, B=0.96 mV).

The FM effect allows the frequency band of carrier signal to broaden due to the frequency swing. Clinically, the most frequently used method for the measurement of frequency swing of ECG is HRV (heart rate variability), and this approach has acquired some achievements [24-26]. We use another parameter defined as

$$Q = \frac{f_0}{BW}, \tag{17}$$

to characterize the frequency swing effect of each spectral harmonic, where f_0 is the central frequency of each harmonic and BW is the 3 dB bandwidth [11,23]. Larger (smaller) Q value indicates a smaller (larger) frequency swing. The calculated Q values for the first five harmonics are 5.5, 11.1, 16.5, 22.3, and 28.1 in sequence.

4.2 Coherence Analysis

For the cardiovascular system, blocked blood vessels, stiff arteries, high peripheral resistance, extruded blood vessel due to damage, blood turbulence, viscous damping, propagation disturbance of arterial pressure pulse, etc., are treated as interferences. They would affect both the blood flow toward its destination and the pressure pulse contour; therefore, they induce various cardiovascular-related diseases. These perturbation signals also interfere with the resonance and coherent oscillation between

the input and the output of the system. In fact, they are equivalent to the noises generated in transmission channel for electronic communication system.

In our research, the cardiovascular system is regarded as an electrically-driven mechanical-pumping system [11]. Thus, the modulated ECG and blood pressure wave are considered as the input and the output signals of the cardiovascular system, respectively. In other words, in such a system the electrical energy is transformed into mechanical power. Now, a cardiovascular system model described in Fig. 13(a) is established based on the concept of modulated ECG, power coherence and perturbation. Moreover, the spectra of modulated ECG including the inter-modulation effect are demonstrated in Fig. 13(b).

Instead of developing complex mathematical equations to characterize the system, we use the coherence function $C_{XY}(f)$, which represents the magnitude squared coherence between input signal X and output signal Y, to quantify the macroscopic effect of power coherence for the system. The function is defined as

$$C_{XY}(f) \equiv \frac{\text{Output power only from input}}{\text{Total output power}}$$

$$= \frac{|P_{XY}(f)|^2}{P_{XX}(f)P_{YY}(f)} \tag{18}$$

where $P_{XX}(f)$ and $P_{YY}(f)$ are the power spectral densities of input and output, respectively, and $P_{XY}(f)$ is the cross power spectral density between input and output [13]. The coherence function always takes on a value in the interval $0 \leq C_{XY}(f) \leq 1$, and with a value close to one, if the perturbation (noise) level is low. When the coherence function is far less than one, it indicates the presence of one or more of the following: (1) a disturbance affecting the output, (2) another input source, or (3) nonlinear relationship between input and output.

Therefore, the function can be used to evaluate the input-output relation of

coherence and extract perturbations between ECG and BPW. Furthermore, the average S of coherence values at the first five harmonic peaks, which constitute most of the energy of the system, is defined as an index for measuring the degree of coherence of the system.

4.3 Experiment and Results

We evaluated the coherence function using the Hamming window with a 600-sample window and an overlap of 500 samples. The estimated coherence functions of a healthy subject and a cardiovascular patient are illustrated in Fig. 14. The fundamental heart frequencies f_0 are 1.1 Hz and 1.35 Hz for the healthy subject and cardiovascular patient, respectively.

Some remarkable differences for the two subjects are summarized as follows:

(1) The average S of coherence values for the first five harmonic frequencies is close to one for the healthy subject, yet approximately 0.85 (<1) for the patient. This means that, for the healthy subject, the input power is coherently coupled to the output and the output is completely dominated by the input, particularly in the first five resonant frequencies (i.e. harmonic frequencies). However, for the patient, perturbations are generated and the output is not entirely determined by the input. In other words, the perturbation signals effectively affect the output.

(2) The bandwidth of coherence function for the first five harmonic peaks is more larger and regular for the healthy subject than that for the patient. This implies that, for the healthy subject, more frequency constituents of the system induce a high coherence value.

(3) The coherence function within the frequency range of slow-varying modulation signals ($\leq 0.4\,\text{Hz}$), in synchrony with respiratory rate, also exhibits a peak for both

the healthy subject and patient. This reveals that the power of such modulation signals is also coherently coupled to the output for both the healthy subject and the patient.

Moreover, the above results are observed not only in the two subjects but also in the experiment in which forty-four subjects participated.

The study subjects were composed of two groups. The first group consisted of 22 healthy subjects (12 males and 10 females, at the ages of 18 to 40) whose health checks are normal and without any reported cardiovascular disease. The second group was composed of 22 patients with cardiovascular-related diseases (13 males and 9 females, at the ages of 36 to 55). The disease patterns were not specified for the study of general effect of coherence function on cardiovascular system. Before the measurement, all the subjects were rested for about twenty minutes to get a steady pulse waveform. The statistical results are demonstrated in box plot in Fig. 15. For healthy subjects, the mean value of S (=0.97) is larger than that (=0.92) for cardiovascular patients. In addition, the small p-value ($= 7.92 \times 10^{-5} < 0.01$) indicates that the coherence values S of healthy subjects and cardiovascular patients are significantly different. Consequently, this index is appropriate for quantifying the coherence characteristic.
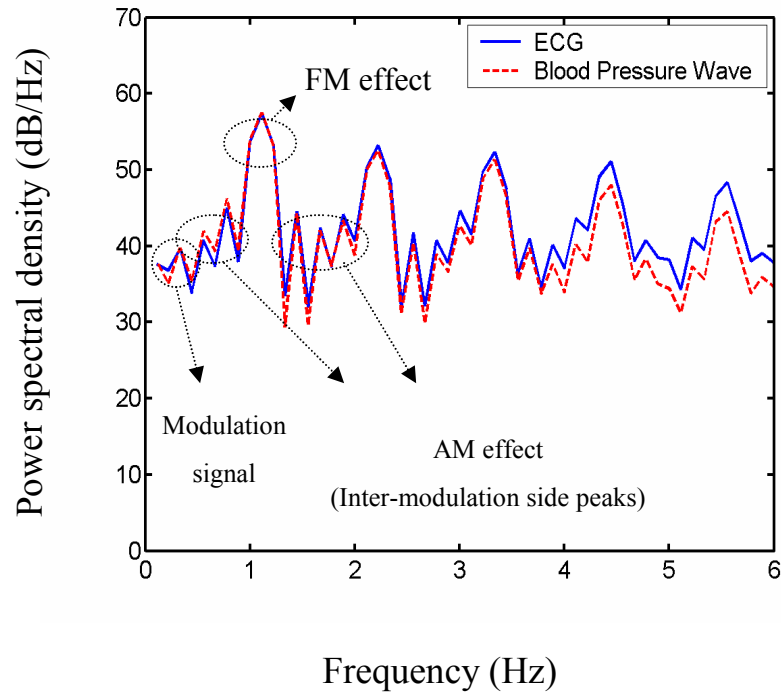
(a)
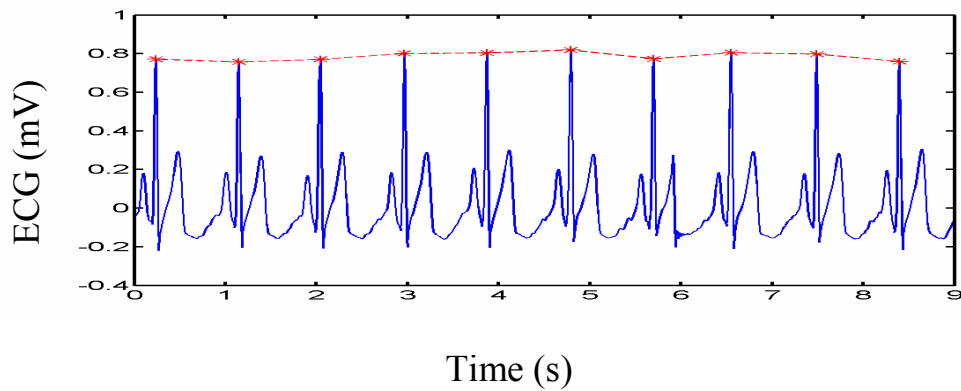
(b)

Fig. 12. (a) The spectra of ECG and blood pressure wave are shown, where the peak in the range of 0 ~ 0.4 Hz is due to the modulation signals and the side peaks around harmonics (sub-harmonics) are attributed to the inter-modulation effect. (b) The peak amplitude variation of the QRS complex wave of modulated ECG, which results from the AM modulation effect, is plotted with a dashed line.
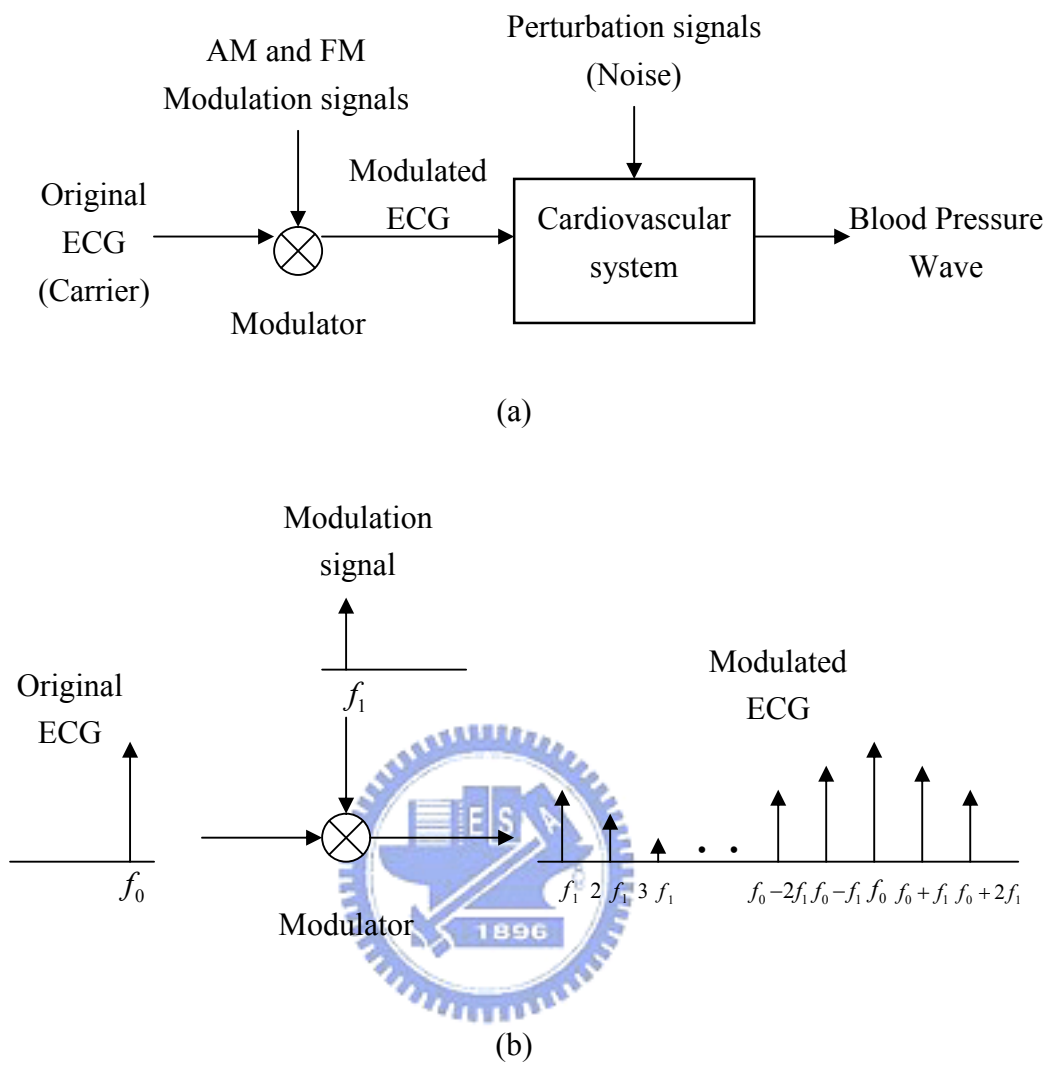
Fig. 13. (a) The presented cardiovascular system model is plotted. (b) The schematic diagram of the spectra of original ECG, modulation signal and modulated ECG is illustrated.
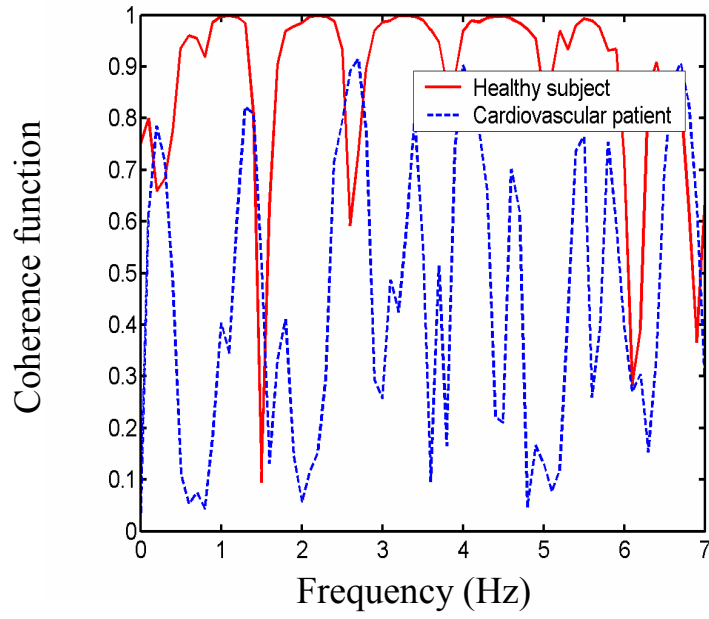
Fig. 14. The coherence functions of a healthy subject and a cardiovascular patient are demonstrated.
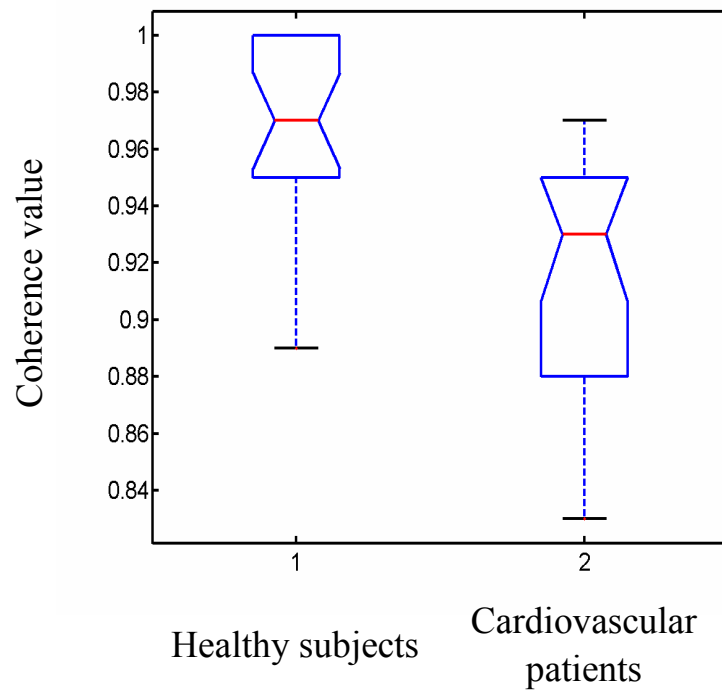
Fig. 15. The statistical results of power coherence index S of twenty-two healthy subjects and twenty-two cardiovascular patients are demonstrated with box plot.

CHAPTER 5.   BLOOD PRESSURE WAVE UNDER MEDITATION

5.1 Time-domain Features of BPW

The blood pressure waveform of the systemic arterial tree is an important determinative of performance of the cardiovascular system. This signal originated by the systole and diastole of the heart conveys such information as the blood ejection ability of the heart, the elasticity of the artery wall, the peripheral resistance, etc. [1]. Abnormality in the blood pressure waveform is linked to various physiological or pathological states such as aging and hypertension [27,28]. Actually, the blood pressure waveform of radial artery detected at wrist is the sphygmographical signal used in Traditional Chinese Medicine (TCM). According to the sphygmographical signal and theory, the clinician of TCM can identify the status of human body and treat the patient.

As more clinical evidences supported the benefits of meditation to health, researchers began investigating the physiological phenomena of human body under meditation some fifty years ago. Dillbeck et al. (1987) compared the physiological differences in two groups of subjects, one under transcendental meditation and the other at rest. Schneider et al. found that the training of transcendental meditation could significantly lower the systolic and diastolic blood pressure of hypertensive persons [29-32]. Meditation hereafter became a feasible method to improve the hypertension. To assess the effect of meditation on the cardiovascular system, this paper presents a quantitative approach for investigating the variation of blood pressure waveform between the pre-meditation and post-meditation sections. We measured the blood pressure waveforms of twenty experimental subjects (Zen-meditation practitioners) and twenty control subjects (normal, healthy subjects

in the same age range as the experimental group). According to the clinical experiences of TCM professionals, we design a set of parameters that quantify the waveform patterns of BPW. The prototype of BPW of a healthy subject is displayed in Fig. 16.

Mechanism of the heart pumping correlating with the BPW is illustrated as follows. The ejection of blood from the left ventricle into the aorta results in the first peak of the BPW that is called the Percussion wave (P wave). The height of P wave, h_1, and the fast ejection time of left ventricle, t_1, are related to the ejection ability of heart and the compliance index of aorta. We define the rising slope of P wave as $\frac{h_1}{t_1}$. A larger slope computed indicates a better performance of the heart ejection function and aorta compliance [33]. Thus it is used as one of the quantitative features to evaluate the cardiovascular system. The second peak, called the Tidal wave (T wave), appears when blood hits the artery wall and rebounds. As a result, T wave is manifest if the artery possesses excellent elasticity that reflects low peripheral resistance of the circulatory system. On the other hand, an artery with stiff wall will make the T wave propagate fast according to the Moens-Korteweg equation of wave velocity [2,34]. Accordingly, the T wave will overlap with the P wave, which results in a wider P wave. The second parameter, $\frac{h_3}{h_1}$, where h_3 represents the height of T wave, is utilized to measure the effect of T wave. We thus expect a large $\frac{h_3}{h_1}$ for an arterial system with better elasticity. The valley height h_4 reveals the level of peripheral resistance [1,33]. As the peripheral resistance increases (decreases), parameter h_4 increases (decreases) as well. The normalized parameter, $\frac{h_4}{h_1}$, is employed to measure

the drift of peripheral resistance. Finally, when the aortic valve is closed, the Dicrotic wave (D wave) is generated. h_5 is the magnitude of D wave and the normalized parameter, $\dfrac{h_5}{h_1}$, represent the effect of D wave on arterial system. Resulting from the stiff aorta or aortic regurgitation, h_5 will decrease.

The peak or valley positions in Fig. 16 demonstrated by crosses are determined by the Matlab program for searching the local maximum or minimum. In this research, the above four parameters, $\dfrac{h_1}{t_1}$, $\dfrac{h_3}{h_1}$, $\dfrac{h_4}{h_1}$ and $\dfrac{h_5}{h_1}$ are used to assess the status of cardiovascular system and the definition of the corresponding parameters are summarized as follows:

$$h_1 = \text{Peak height of P wave} - \text{Valley height of } V_1 \tag{19}$$

$$h_3 = \text{Peak height of T wave} - \text{Valley height of } V_1 \tag{20}$$

$$h_4 = \text{Valley height of } V_3 - \text{Valley height of } V_1 \tag{21}$$

$$h_5 = \text{Peak height of D wave} - \text{Valley height of } V_3 \tag{22}$$

$$t_1 = \text{Time of } V_1 - \text{Time of Peak of P wave} \tag{23}$$

$$\text{Variation percentage} = \frac{\eta_{post-meditation} - \eta_{pre-meditation}}{\eta_{pre-meditation}}, \tag{24}$$

where η denotes one of the four parameters, $\dfrac{h_1}{t_1}, \dfrac{h_3}{h_1}, \dfrac{h_4}{h_1} or \dfrac{h_5}{h_1}$. To avoid null denominator caused by the disappearance of *pre-meditation* T wave (in the case, $h_3=0$), the variation percentage of $\dfrac{h_3}{h_1}$ is defined to be zero if T wave is absent before and after the meditation. On the other hand, if T wave exists only after meditation, the variation percentage of $\dfrac{h_3}{h_1}$ will be assigned to 100% to avoid infinity.

5.2 Experiment and results

The four parameters, $\frac{h_1}{t_1}$, $\frac{h_3}{h_1}$, $\frac{h_4}{h_1}$ and $\frac{h_5}{h_1}$ are averaged during the 10-seconds time interval, respectively. The study subjects were composed of two groups. The control group consisted of 20 normal subjects (11 males and 9 females, at the ages of 18 to 25). The experiment group consisted of 20 Zen-Buddhist meditation practitioners (7 males and 13 females, at the ages of 20 to 40). Their experiences in Zen-Buddhist practice span 6.9 ± 3.3 years. The meditators practiced Zen-Buddhist meditation for 40 minutes. During the meditation session, the subjects sat, with eyes closed, in the full-lotus or half-lotus position. The control subjects just sat in a relaxation position for the same recording interval. The blood pressure waveforms were recorded before and after the meditation.

Figure 17 illustrates an example of the blood pressure waveform of an experimental subject. The solid (dashed) curve shows the *pre-(post-)meditation* BPW. In Fig.17, *post-meditation* P wave rises more steeply than the *pre-meditation* one. For this particular subject, poor arterial elasticity makes the *pre-meditation* T wave occur earlier and merge with P wave, resulting in a broadened P wave. As for the *post-meditation* BPW, T wave becomes evident and distinguishable from P wave, inferring the enhanced arterial elasticity as a consequence of the meditation practice. Moreover, the V_3 valley descends (i.e., h_4 decreases) after meditation, indicating the decrease of peripheral resistance. And the magnitude of D wave is strengthened after meditation. In sum, the *post-meditation* BPW entirely reflects a more robust cardiovascular system which could be tuned up to by the Zen meditation.

The statistical results of forty subjects are demonstrated in Table 4. In comparison with the control group, Zen-meditation practitioners have higher ranges of variation

percentages in all four parameters. Next, we describe the performance of each parameter in detail. Consider the rising slope of P wave, $\dfrac{h_1}{t_1}$, that reflects the ejection ability of left ventricle or aorta elasticity. The experimental group has the group mean increase from 390.8 to 435.1, a variation percentage of 11.7%, that is 5% higher than the variation percentage of control group. The second parameter $\dfrac{h_3}{h_1}$, measuring the effect of T wave, especially demonstrates distinct enhancement of the arterial elasticity in the experimental group (three times the increasing rate of the control group). We discover that, even though some experimental subjects might have vague T wave, Zen meditation often boosted the T wave. Next, the high decreasing rate of $\dfrac{h_4}{h_1}$ reveals the reduced peripheral resistance after meditation. Finally, the increasing $\dfrac{h_5}{h_1}$ infers that Zen meditation significantly improves the quality of semilunar valves and artery elasticity. To show the statistical significance of discriminating between two groups, we evaluate the P values for the variation percentage of each parameter. All the P values are smaller than 0.05, further corroborating the significant distinction of improvement between two groups. In comparison with normal relaxation, Zen meditation effectively improve the characteristics of cardiovascular system according to the set of parameters extracted from the blood pressure wave.

Why can meditation improve the cardiovascular system? The possible reason could be stated as follows. In meditation, the meditator devotes the attention to his breath; thus the meditation process reduces the dispersive thought, brain activity, muscle stress and the influence of sympathetic system on blood vessels. Consequently, the artery wall becomes more relaxed and elastic. In other words, the blood flow will

encounter less peripheral resistance and could be well transported into organ, tissue, cell, etc. Under the high-efficiency blood transporting system, human health will be improved.

Recently, complementary and alternative medicine has interested the researchers to investigate its effect based on scientific evidence. It is no doubt that meditation plays an important role in these corresponding fields. In this paper, we have reported our investigation of the on-the-spot effect of Zen meditation on the cardiovascular characteristics, with the control group involving the same number of normal, healthy subjects within the similar age range. We analyzed the on-the-spot variations because of the difficulty of controlling the open-system experimental conditions for human subjects.

In the modern society, the cardiovascular related diseases have become a dominant cause of death for a long time. Meditation provides an alternative way of healthcare when the conventional treatment encounters the bottleneck. As a consequence, it urges the development of scientific approach to the underlying mechanism and the effects on human life system. More scientific and clinical evidences disclosed may inject innovative thoughts into the mainstream medicine and the popular healthcare routine. According to our preliminary results of analyzing the BPWs, Zen meditation produces more effective improvement in the cardiovascular characteristics than normal relaxation.
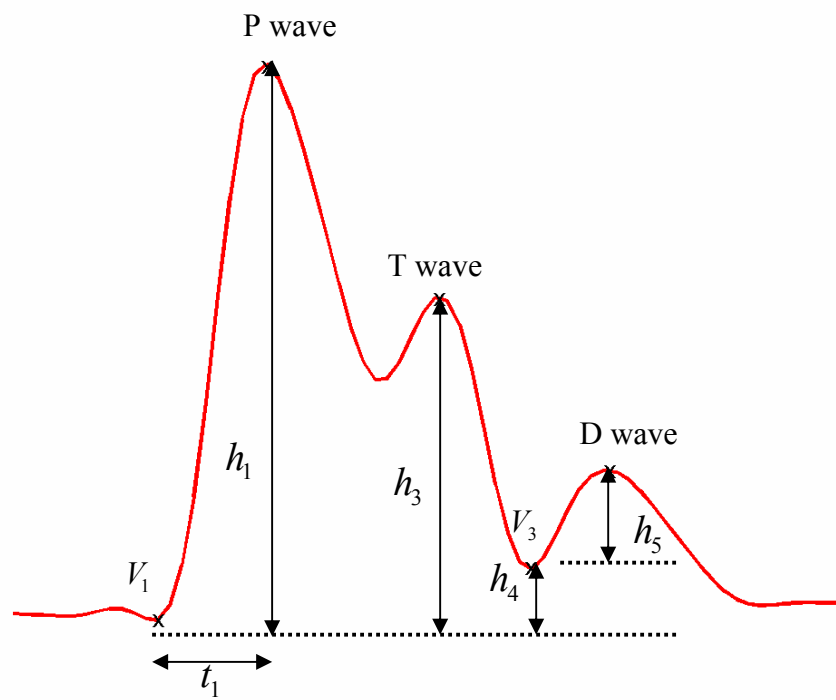
Fig. 16. Prototype of a normal blood pressure waveform (BPW).
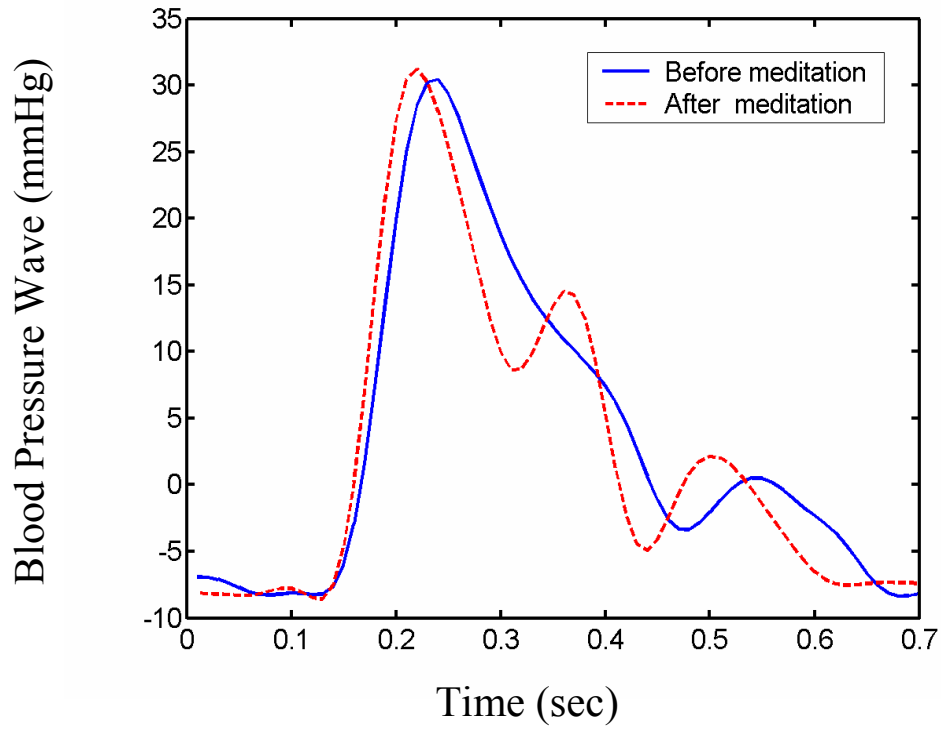
Fig. 17. The *pre-meditation* (solid curve) and *post-meditation* (dashed curve) BPW for an experimental subject.

Table 4. The statistical results of four parameters ($\frac{h_1}{t_1}$, $\frac{h_3}{h_1}$, $\frac{h_4}{h_1}$, $\frac{h_5}{h_1}$) and their variation percentages. P values are evaluated to show the statistical significance of discrimination between two groups.

		$\dfrac{h_1}{t_1}$	$\dfrac{h_3}{h_1}$	$\dfrac{h_4}{h_1}$	$\dfrac{h_5}{h_1}$
Control group	*Pre-Meditation* (Mean±Std.)	380.6 ± 26.0	0.21 ± 0.19	0.27 ± 0.08	0.13 ± 0.04
	Post- Meditation (Mean±Std.)	405.7 ± 25.3	0.25 ± 0.19	0.24 ± 0.07	0.15 ± 0.07
	Variation percentage	6.7%	13.0%	-9.3%	14.2%
Meditators	*Pre-Meditation* (Mean±Std.)	390.8 ± 28.0	0.20 ± 0.19	0.25 ± 0.09	0.13 ± 0.04
	Post- Meditation (Mean±Std.)	435.1 ± 18.9	0.36 ± 0.13	0.22 ± 0.08	0.16 ± 0.03
	Variation percentage	11.7%	41.2%	-13.5%	27.9%
P value		0.005 (< 0.05)	0.026 (< 0.05)	0.032 (< 0.05)	0.029 (< 0.05)

CHAPTER 6.   CONCLUSION AND DISCUSSION

Advancement of hemodynamics enables researchers to verify the resonance phenomenon in blood circulation The model of BPW can elaborate the following physiological phenomena, which are hard to be explained by the traditional theory of blood flow,

(1) With a small power (1.7W), the heart can push the blood to circulate all over the body day and night.

(2) The arch of aorta have a turn of 180 degrees.

(3) The blood can enter the organ which couple to the aorta with 90 degrees.

From the evolutionary viewpoint, resonance, corresponds to the most efficient energy transfer state of a system. It also enables the living beings to compete in the nature. On the other hand, if a system deviates from its resonance state, diseases or death often arise.
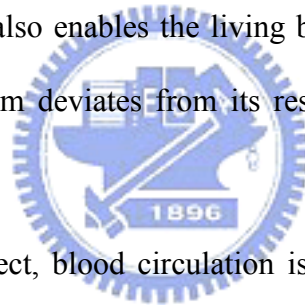
From the macroscopic aspect, blood circulation is viewed as a forced oscillation which is electrically driven by the heart. In spite of the quite distinct wave patterns in the time domain, the power spectra of the ECG and BPW overlap well for the normal, healthy subjects, yet deviate significantly for the patients with vascular-related diseases. The results conform to the concept of *frequency matching* and imply that there are close spectral relationships and information shared between the ECG and the BPW, which can be used to measure the condition of blood circulation. The correlation coefficient estimated for the frequency band 0-20Hz further reflects much weaker coupling efficiency in the ECG-to-BPW system for the abnormal subjects (mean = 0.542) in comparison with the normal subjects (mean = 0.821). In the bicoherence analysis, a diseased circulation system exhibits poor cross

quadratic-phase coupling between ECG and BPW (healthy subjects: 0.828 > vascular patients: 0.619). Furthermore, the result of transfer function analysis for the patients indicates a low energy transmission efficiency from input to output (S.D. of healthy subjects: 0.206 < vascular patients: 0.301). In addition, we propose a frequency-domain equivalent circuit to model the blood circulation, and develop the quality factor (Q) to assess the resonance characteristic of each harmonic-related resonator. The results reveal that the patients who have poor coupling efficiency from the heart also tend to have poor resonance in their circulatory system (healthy subjects vs. vascular patients, f: 5.68 > 5.38, 2f: 10.59 > 9.77, 3f: 15.45 > 13.99, 4f: 20.65 > 18.19, 5f: 27.35 >24.19).

Why does a mechanical vibration signal (BPW) have almost the same spectral components as an electrophysiological signal (ECG) in a healthy cardiovascular system? We hypothesize that the BPW, transduced from the ECG of the heart, is optimally coupled from the heart to the arterial system due to the superior elasticity of the vessels. The spectral contents are thus preserved in the circulation under the well-elastic arterial system since the pressure wave encounters little perturbation, less reflection, and smaller peripheral resistance. Considering the circulatory system modeled as an electrically-driven, mechanical-pumping system, we developed several methods to quantitatively evaluate the effects of spectral coupling and resonance between ECG and BPW, in which the ECG and BPW represent, respectively, the electrically driving source and the mechanically responding output.

Next, Using coherence function analysis, we found that for healthy subjects, most spectral components of the input (ECG) are coherently coupled to those of the response (BPW) (S=0.97), so that less perturbation is found. On the other hand, for cardiovascular patients, the influence of perturbation signals on the output is relatively

important (S=0.92). In other words, the perturbation signals seriously interfere with the coherence power transfer. If S approaches one, the perturbation effect becomes smaller. The cardiovascular system can thus be maintained in a better condition. On the contrary, if S deviates from one, severe perturbation occurs in the cardiovascular system that will decay fast.

Although we cannot identify the perturbation source using the model, this method provides an approach for quantifying such macroscopic phenomenon as the coherence power transfer and perturbation in the system. Moreover, we have demonstrated that cardiovascular system exhibits some phenomena similar to the technologies and mechanisms employed in communication systems, for example, the FM and AM schemes. These analogies give us more insight into the cardiovascular system. In summary, the results provide us with a new scope to study blood circulation using power coherence. Due to the close relationship between spectral harmonics and various organs, this approach might be extended to the study of organ disease [11]. Cardiovascular-related diseases have been one of the major causes of death. Furthermore, they often cause sudden death without warning. To identify the early sign of disease in advance, cardiovascular system characterization by spectral analysis may offer a non-invasive and affirmative approach for medical prognosis.

REFERENCES

[1] W. R. Milnor, Hemodynamics, 2nd ed. Baltimore, MD: Williams & Wilkins Co, 1989.

[2] W. W. Nichols and M. F. O'Rourke, McDonald's Blood Flow in Arteries, Philadelphia: Lea & Fegiber, 1990.

[3] Y. Y. Lin Wang, M. Y. Jan, C. S. Shyu, C. A. Chiang and W. K. Wang, "The natural frequencies of the arterial system and their relation to the heart rate," IEEE Trans. Biomed. Eng., vol. 51, pp. 193-195, 2004.

[4] Y. Y. Lin Wang, W. C. Lia, H. Hsiu and M. Y. Jan, "Effect of length on the fundamental resonance frequency of arterial models having radial dilation," IEEE Trans. Biomed. Eng. vol. 47, pp. 313-318, 2000.

[5] W. K. Wang, Y. Y. Lo, T. L. Hsu, and Y. Y. Wang Lin, "Resonance organ with heart," in Proceedings of the International Symposium on Biomedical Engineering, Singapore, edited by W. J. Young (Hemisphere publishing corp., New York) pp. 259-297, 1989.

[6] Y. Y. Lin Wang, S. L. Chang, Y. E. Wu, T. L. Hsu, and W. K. Wang, "Resonance: the missing phenomenon in hemodynamics," Circ. Res. vol. 69, pp. 246-249, 1991.

[7] G. L. Yu, Y. Y. Wang Lin, and W. K. Wang, "Resonance in the kidney system of rats. American Journal of Physiology (Heart Circ. Physiol.), vol. 267, H1544-H1548, 1994.

[8] W. K. Wang, T. L. Hsu, H. C. Chang, and Y. Y. Lin Wang, "Effect of acupuncture at hsien-ku (ST-43) on the pulse spectrum and a discussion of the evidence for

the frequency structure of Chinese medicine," Am. J. Chin. Med. vol. 26, No. 1, pp. 73-82.

[9] X. C. Chang, Studies on the relationship between Chinese medical physiology and organ resonance theory- from the viewpoint of pulse spectrum analysis, Dr. Thesis, Institute of Chinese medical science, Dr. Thesis, China Medical University, Taichung, 1993.

[10] S. S. Rao, Mechanical vibrations, N. J. : Prentice Hall, 2004.

[11] C. C. Wei, P. C. Lo, and L. K. Wu, "Spectral Analysis of the Blood Circulation Based on the Viewpoint of Resonance," Jpn. J. Appl. Phys., 2005. (accepted)

[12] Y. Y. L. Wang, C. C. Chang, J. C. Chen, H. Hsiu, and W. K. Wang, "Pressure Wave Propagation in a distensible tube arterial model with radial dilation," IEEE Engineering in Med. Bio. Mag., pp. 51-56, Jan. 1997.

[13] R. Johansson, System Modeling and Identification, Englewood Cliffs, N.J.: Prentice Hall, 1993.

[14] C. L. Nikias and A. P. Petropulu, High-order spectra analysis: A Nonlinear Signal Processing Framework, Englewood Cliffs, N.J.: Prentice Hall, 1993.

[15] C. L. Nikias and M. R. Raghuveer, "Bispectrum estimation: a digital signal processing framework," Proc. IEEE, vol. 75, no. 7, pp. 869-891, 1987.

[16] P. J. Huber, B. Kleiner, T. Gasser, and G. Dumermuth, "Statistical methods for investigating phase relations in stationary stochastic process," IEEE Trans. Audio Electroacoustics , vol. 19, pp.78-86, 1971.

[17] J. Jamesek, A. Stefanovska, and P. V E McClintock, "Nonlinear cardio-respiratory interactions revealed by time-phase bispectral analysis," Phys. Med. Biol., vol. 49, No. 18, pp. 4407-4425, 2004.

[18] J. W. A. Fackrell, P. R. White, J. K. Hammond, and R. J. Pinnington, "The interpretation of the bispectra of vibration signals-I. theory," Mech. Syst. Signal Pr., vol. 9, pp. 257-266, 1995.

[19] J. W. A. Fackrell, P. R. White, J. K. Hammond, and R. J. Pinnington, "The interpretation of the bispectra of vibration signals-II. Experimental results and applications," Mech. Syst. Signal Pr., vol. 9, pp. 267-274, 1995.

[20] P. A. Rizzi, Microwave Engineering: passive circuits, Prentice-Hall, Englewood Cliffs, N. J., 1988.

[21] G. B. Moody, R. G. Mark, A. Zoccola, and S. Mantero, "Derivation of respiratory signals from multi-lead ECGs," Computers in Cardiology, vol. 12, pp. 113-116, 1985.

[22] F. Pinciroli, R. Rossi, and L. Vergani, "Detection of electrical variation for extraction of respiratory information," Computers in Cardiology, vol. 2, pp. 499-502, 1985.

[23] F. R. Dungan, Electronic communications systems, Albany, N.Y.: Delmar Publishers Inc., 1993.

[24] M. S. Houle, and G. E. Billman, "Low-frequency component of the heart rate variability spectrum: a poor marker of sympathetic activity," American Journal of Physiology (Heart and Circulatory Physiology) vol. 45, pp. 215-223, 1999.

[25] S. C. Malpas, B. L. Leonard, S. J. Guild, J. V. Ringwood, M. Navakatikyan, P. C. Austin, G. A. Head, and D. E. Burgess, "The sympathetic nerves system's role in regulating blood pressure variability," IEEE Eng. Med. Biol. Mag. Vol. 20, pp. 17-24, 2001.

[26] R. J. Leor-Librach, S. Eliash, E. Kaplinsky, and B. Z. Bobrovsky, "Very

low-frequency heart rate variability wave amplitude and sympathetic stimulation-characterization and modeling," IEEE Trans. Biomed. Eng. vol. 50, pp. 797-803, 2003.

[27] J. N. Cohn, S. Finkelstein, G. Mcveigh, D. Morgan, L. Lemay, J. Robinson and J. Mock, "Noninvasive pulse wave analysis for the early detection of vascular disease," Hypertension vol. 26, pp. 503-508, 1995.

[28] G. E. Mcveigh, C. W. Bratteli, D. J. Morgan, C. M. Alinder, S. P. Glasser, S. M. Finkelstein and J. N. Cohn, "Age-related abnormality in arterial compliance identified by pressure contour analysis," Hypertension vol. 33, pp.1392-1398, 1999.

[29] R.H. Schneider, F. Staggers, C. N. Alexander, W. Sheppard, M. Rainforth , K. Kondwani, S. Smith and C. G. King, "A randomized controlled trial of stress reduction for hypertension in older African Americans," Hypertension vol. 26, pp. 820-827, 1995.

[30] V. A. Barnes, H. C. Davis, J. B. Murzynowski and F. A. Treiber, "Impact of meditation on resting and ambulatory blood pressure and heart rate in youth. Psychosom," Med. vol. 66, pp. 909-914, 2004.

[31] C. N. Alexander, R. H. Schneider, W. Sheppard, B. M. Clayborne, M. Rainforth, J. Salerno, K. Kondwani, S. Smith, K. G. Walton and B. Egan, "Trial of stress reduction for hypertension in older African Americans," Hypertension vol. 28, pp. 228-237, 1996.

[32] A. Castillo-Richmond, R.H. Schneider, C.N. Alexander, R. Cook, H. Myers, S. Nidich, C. Haney, M. Rainforth and J. Salerno, "Effects of stress reduction on

carotid atherosclerosis in hypertensive African Americans," Stroke vol. 31, pp. 568-573, 2000.

[33] J. F. Fey, Contemporary Sphygmology in Traditional Chinese Medicine, Beijing : People's Medical Publishing House, 2003, pp. 162-164.

[34] A.W.Khir, and K.H. Parker, "Measurement of wave speed and reflected waves in elastic tubes and bifurcations," Journal of Biomechanics vol. 35, pp. 775-783, 2002.

博士候選人資料

姓　名　：魏清泉

性　別　：　男

出生年月日 ： 民國 55 年 12 月 26 日

籍　貫　：　南投縣草屯鎮中正路 808 號

學　歷：國立交通大學電信工程系畢業（75 年 9 月 ～ 79 年 9 月）

　　　　國立交通大學電信工程研究所畢業(79 年 9 月~81 年 9 月)

　　　　國立交通大學電信工程研究所博士班(90 年 9 月~95 年 1 月)

經　歷　：　建國科技大學電子工程系講師（83 年 9 月 ~）

論文題目　：基於諧振與同調觀點之血液壓力波分析